MATERIALS CHEMISTRY FRONTIERS

REVIEW

View Article Online
View Journal | View Issue

Cite this: *Mater. Chem. Front.*, 2024, **8**, 930

Recent advances in red-emissive carbon dots and their biomedical applications

Weixia Qin,[a] Meiyan Wang,[a] Yan Li,[a] Longchuang Li,[a] Khurram Abbas,[b] Zijian Li,[a] Antonio Claudio Tedesco [bc] and Hong Bi *[a]

Recently, there has been a lot of interest in the use of red-emissive carbon dots (R-CDs) due to their low toxicity, solubility in water, and excellent optical properties. These properties make them perfect for use in various biomedical applications. One of the main advantages of R-CDs is that they can penetrate deep into biological tissue without any interference from the tissue's fluorescence. More and more studies have been conducted to explore the potential applications of R-CDs in medicine, making them an exciting area of research. However, one of the challenges is preparing R-CDs with a high fluorescence quantum yield in the deep-red or near-infrared region, and this is still a significant hurdle. Therefore, it is crucial to investigate the preparation approaches of R-CDs with high quantum yield, narrow emission, and multi-functionality to overcome this challenge. This review aims to discuss the synthetic strategies, optical properties, and potential biomedical applications of R-CDs. The focus will mainly be on the research progress of their applications in biological imaging, tumor photodynamic/photothermal therapy, and in the field of synergistic therapy. Additionally, we will also discuss the challenge of achieving R-CDs with specific properties favorable for prospects in biomedical applications.

Received 1st September 2023,
Accepted 6th December 2023

DOI: 10.1039/d3qm00968h

rsc.li/frontiers-materials

1. Introduction

Carbon dots (CDs), which are zero-dimensional carbon-based nanomaterials with ultrafine sizes of less than 10 nm, are promising candidates for various applications. Due to their distinctive optical properties, low toxicity, and the availability of raw materials for creating them, they have received substantial attention. The main forms include graphene quantum dots (GQDs), carbon quantum dots (CQDs), carbon nanodots (CNDs), and carbonized polymer dots (CPDs).[1–5] GQDs are highly crystalline graphene sheets with regular structures, including single, double, and multi-layered structures. It has been reported that GQDs can be prepared in 1–2 layers, which have good multi-colored emission, photostability, biocompatibility, chemical inertness, and other advantages. CQDs,

[a] School of Materials Science and Engineering, Anhui University, 111 Jiulong Road, Hefei 230601, China. E-mail: bihong@ahu.edu.cn
[b] School of Chemistry and Chemical Engineering, Anhui University, 111 Jiulong Road, Hefei 230601, China
[c] Department of Chemistry, Center of Nanotechnology and Tissue Engineering-Photobiology and Photomedicine Research Group, Faculty of Philosophy, Sciences and Letters of Ribeirão Preto, University of São Paulo, Ribeirão Preto, São Paulo 14040-901, Brazil

Weixia Qin

Weixia Qin received her BS degree in Polymer Materials and Engineering from Shandong First Medical University in 2022 and is now pursuing her MS degree under the supervision of Prof. Hong Bi from the School of Materials Science and Engineering, Anhui University. Currently, her main research interests are in the synthesis of red-emissive carbon dots and their application in bioimaging.

Meiyan Wang

Meiyan Wang received her BS degree in Applied Chemistry from Wanxi College in 2022. She joined the School of Materials Science and Engineering of Anhui University in 2022 to pursue her MS degree under the supervision of Prof. Hong Bi with her main research interest in the synthesis of carbon dots and their application in photodynamic anti-bacteria.

however, contain a large amount of amorphous carbon and have a spherical nanoparticle structure. GQDs and CQDs are comprised of sp^2-hybridized carbon nanocrystals and have rich functional groups on their surface.[2,6] The special functional groups, such as the amino group, carboxyl group, and hydroxyl group on the surface of the carbon core can regulate the optical properties of CDs and their solubility in different solvents.[7] The structure and properties of CDs are closely related to the selection of reaction precursors and their molar ratios, dispersion solvents, heteroatom doping process, *etc.* Many studies have shown that CDs' structure, size, and surface functionalized groups can be effectively regulated by controlling different reaction conditions; thus, CDs with unique chemical and physical properties can be prepared.[8]

In 2004, Xu *et al.* discovered CDs during the arc discharge method preparation of single-walled CNTs (SWCNTs).[9] Due to their excellent optical properties, resistance to photobleaching and good biocompatibility, CDs have attracted significant interest from researchers and since then the study of CDs has developed rapidly (Fig. 1). In 2006, CDs were synthesized by laser ablation and, for the first time, simple organics were attached to acid-treated carbon nanoparticles by surface passivation to improve their surface properties for multi-colored photoluminescence (PL).[10] In 2007, Liu *et al.* reported for the first time the preparation of small (<2 nm) multicolor fluorescent CDs from candle-burning soot and the use of purified CDs for polyacrylamide gel electrophoresis.[11] This was the first attempt to prepare CDs using a bottom-up approach, laying the foundation for efficiently preparing red-emissive carbon dots (R-CDs). In 2009, CDs were successfully used for *in vivo* imaging, and this work confirmed the promising application of CDs in biomedical fields.[12]

In the early stage of CD research, most CDs exhibited blue or green fluorescence. It was impossible to avoid interference from the biological tissue's fluorescence during bioimaging, which could lead to poor tissue penetration.[13] Moreover, high levels of photon scattering and light absorption often limit the depth of penetration. In contrast, R-CDs prepared by elaborate design (*e.g.* selection of suitable precursor materials, dispersants, and advantageous synthesis conditions) can effectively eliminate autofluorescence interference and improve the imaging signal-to-noise ratio.[14] In addition, researchers have also

Yan Li

Li Yan received her BS degree in Polymer Materials and Engineering from the First Medical University of Shandong, China in 2022. Now, she is a Master's student under the supervision of Prof. Hong Bi at Anhui University. Her research is now focused on the synthesis of novel carbon dots and their anti-oxidation activity studies.

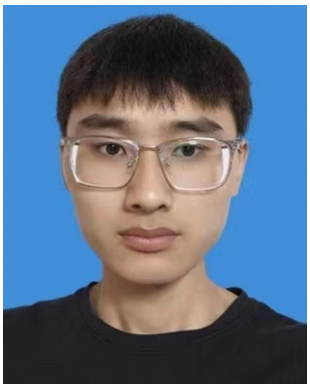

Longchuang Li

Li Longchuang received his BS degree from Bengbu University in 2022. He is currently a Master's student at Anhui University under the supervision of Prof. Hong Bi. His main research interests are the synthesis of high-quality carbon dots and a study on their electroluminescent properties.

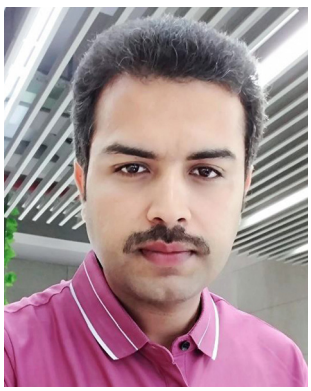

Khurram Abbas

Khurram Abbas completed his BS degree in Chemistry from Islamia College Peshawar, Pakistan, in 2015 and received a MS degree in Biochemistry from the Institute of Chemical Sciences, University of Peshawar, Pakistan, in 2019. Currently, he is pursuing his PhD under the supervision of Prof. Hong Bi. His research is mainly focused on the synthesis of novel carbon dots and exploring their potential application in anti-oxidation and anti-aging area.

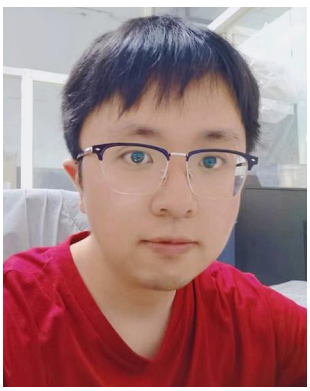

Zijian Li

Zijian Li is currently an associate professor at the School of Materials Science and Engineering, Anhui University, P. R. China. He received his PhD in chemistry from the University of Science and Technology of China in 2019 and then moved to the China Academy of Engineering Physics to work as a postdoctoral researcher on energetic materials. His current research interests are focused on the synthesis of carbon dots with tailored properties as well as exploring their applications in biology and light-emitting devices.

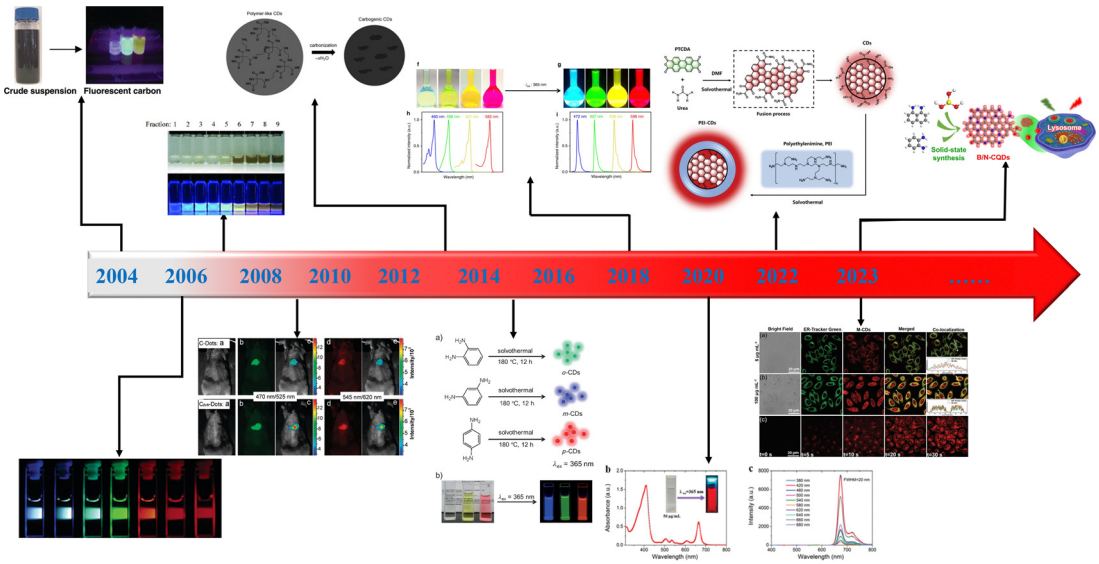

Fig. 1 Development timeline of fluorescent CD research. Reprinted with permission from ref. 9, 10, 12 and 22, Copyright 2004, 2006, 2009, and 2023, American Chemical Society; ref. 11, 15, 18, 20, 21 and 23, Copyright 2007, 2013, 2015, 2020, 2022, and 2023 Wiley-VCH Verlag GmbH & Co. KGaA, Weinheim; ref. 19, Copyright 2018, Nature Publishing Group.

attempted to modulate the energy level of CDs through doping and surface modification to promote the red-shift of their emission wavelengths, which has also significantly contributed to the rapid development of R-CD research. In 2013, polymers were used as precursors for the first time in the preparation of R-CDs, a breakthrough in extending the range of synthetic precursors for R-CDs from small molecules and inorganic carbon materials to polymers, leaping from graphite and small molecules to cross-linked polymeric materials.[15] In 2014, Hao *et al.* could regulate the PL emission of CDs to 650 nm by adjusting the excitation wavelength,[16] Qu *et al.* reported R-CDs with three primary colors luminescence and the longest emission up to 650 nm.[17] In 2015, Jiang *et al.* successfully produced R-CDs with an excitation-independent emission at 604 nm using *p*-phenylenediamine (*p*-PD) as precursors.[18] In 2018, Fan and co-workers synthesized triangular CQDs (T-CQDs) using a facile solvothermal method with resorcinol as the carbon source. They achieved multi-colored luminescence from blue to red with very narrow emissions.[19] In 2020, Yang and co-workers reported the fabrication of red-emissive carbonized polymer dots (CPDs) with a narrowest full width at half maximum (FWHM) of 20 nm from the leaves of the Redbud species using solvothermal synthesis, which not only demonstrated the new polymeric properties of CPDs, but also provided a new crimson-emitting nanomaterial for biomedical applications and optoelectronic devices.[20] With continuous improvement in the structural design and synthetic routes of R-CDs,[21] they are gradually being widely used in bio-imaging, organelle targeting, tumor phototherapy and drug delivery, promoting the development of nanomaterials in the biomedical field, as shown in Fig. 1.

In recent years, there has been a significant increase in research on R-CDs. Because most R-CDs show excitation-dependent

Antonio Claudio Tedesco

Antonio C. Tedesco is currently a full Professor at São Paulo University, Center of Nanotechnology &Tissue Engineering Photobiology and Photomedicine Research Group FFCLRP, Ribeirão Preto, SP, Brazil. His main research interests are in the fields of the photodynamic therapy nanotechnology and tissue engineering, as well as exploring new photoactive molecules and a new drug delivery system for cancer and neurodegenerative disease treatment.

Hong Bi

Hong Bi is currently a full Professor at the School of Materials Science and Engineering of Anhui University, China. Her research interests focus on the chemical synthesis of fluorescent carbon dots and their bio-applications, such as live cell imaging, anti-oxidation, and photodynamic therapy of tumors. She has given more than 22 invited talks at international and national conferences and co-authored 138 peer-reviewed papers with a total of more than 4,400 citations and an H-index of 35. Besides, she has 21 Chinese National Invention Patents and 1 Netherland Patent authorized.

emissions and low fluorescence quantum yields, well designing the structure is crucial by carefully selecting the precursors and controlling R-CDs' synthesis conditions. This review briefly describes the recent progress in research on the synthesis and optical properties of R-CDs, highlighting new advances in bioimaging and tumor therapy. The prospects and challenges for developing R-CDs in biomedical areas are also discussed.

2. Synthetic strategies of R-CDs

Generally, preparation strategies for CDs consist of top-down and bottom-up methods. In the top-down approach, the original non-luminescent carbon materials (graphite, graphene oxide, carbon black, activated carbon, carbon nanotubes, *etc.*) are mainly used and subjected to relatively severe external conditions such as electrochemical exfoliation, laser ablation, chemical oxidation, and arc discharge to cut large carbon materials into small carbon particles less than 10 nm in size.[24–27] The top-down synthesis strategy realizes the conversion of multi-dimensional carbon materials to zero-dimension, further expanding the carbon research field. However, the limited options of raw materials, complicated preparation processes, and relatively low product yields lead to the high cost of CD preparation through the top-down method. Moreover, it usually requires an additional step for surface functionalization or passivation of the CDs obtained in this way if specific functionalities for biological applications are demanded.

On the other hand, the bottom-up method mainly uses small organic molecules or biomass containing organic molecules as precursors, which can be carbonized by hydrothermal/solvothermal processes, microwave-assisted heating, or high-temperature pyrolysis. Once separated and purified, the fluorescent CDs will be obtained.[28,29] A variety of precursor options might be the most attractive advantage of the bottom-up synthesis of CDs, which allows the designed functionalities or surface passivation of CDs to be accomplished in a one-pot synthesis with relatively high yields.[30] However, it is also faces the problems of various by-products, tedious purification processes, and non-negligible batch differences. Therefore, realizing CDs' large-scale and controlled synthesis is still a great challenge in this emerging area.

2.1 Top-down

2.1.1 Laser ablation. Laser ablation is a method that uses high-energy laser beams in the range of 193 nm to 1064 nm to irradiate bulk carbon-containing material so that small carbon fractions are removed from it to form CDs. However, the operation of this method is too complex, as it requires laser irradiation, oxidation, and a passivation process during the whole process. As a result, the yield and purity of the prepared CDs are usually behind some standard conditions, and the particle size is not uniform.

Yang *et al.* used the pulsed laser ablation method to synthesize CNDs from a graphite target in ethanol. The obtained CNDs were well-dispersed nanoparticles with a diameter size of 3–6 nm. The HRTEM image showed that the CNDs had clear lattice fringes with a lattice spacing of 0.204 nm (Fig. 2a–d).[31] The use of one-step pulsed laser ablation associated with the choice of precursors could be described as a green technology to obtain CDs. The method can be used directly without separation or further purification from organic solvents. Dating back to 2006, Sun *et al.* used graphite powder as a carbon source, argon and water vapor as protective gas, irradiation with a Nd:YAG laser (1064 nm, 10 Hz), treatment with 2.6 mol L^{-1} nitric acid solution to obtain 3–12 nm carbon nanoparticles, and then passivated these with polyethylene glycol (PEG) or PEI, to finally obtain blue-, green-, and red-emissive CDs (Fig. 2d and e).[10]

2.1.2 Electrochemical synthesis. During the electrochemical synthesis, conductive carbon materials are used as electrodes to prepare CDs. In this method, controlled synthesis of CDs can be achieved by controlling the voltage and current intensity applied. Kang and co-workers proposed a simple electrochemical method for the large-scale synthesis of high-purity CDs in

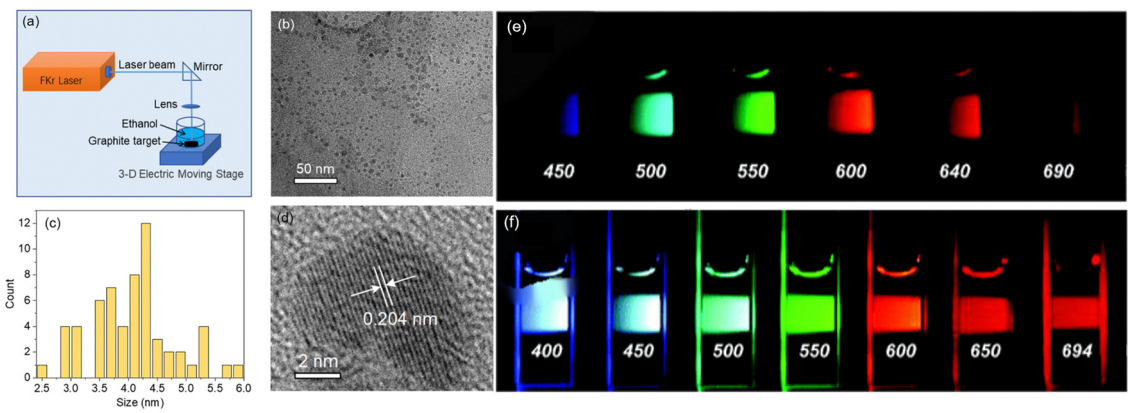

Fig. 2 (a) PLA setup for the preparation of CNDs in ethanol. (b) TEM image of the CNDs. (c) Size distribution of the CNDs. (d) HRTEM image of a single CND. Reprinted with permission from ref. 31, Copyright 2021, Wiley-VCH Verlag GmbH & Co. KGaA, Weinheim. (e) 400 nm excitation through the band-pass filter at different wavelengths. (f) Excited at the displayed wavelength and photographed directly. Reprinted with permission from ref. 10, Copyright 2006, American Chemical Society.

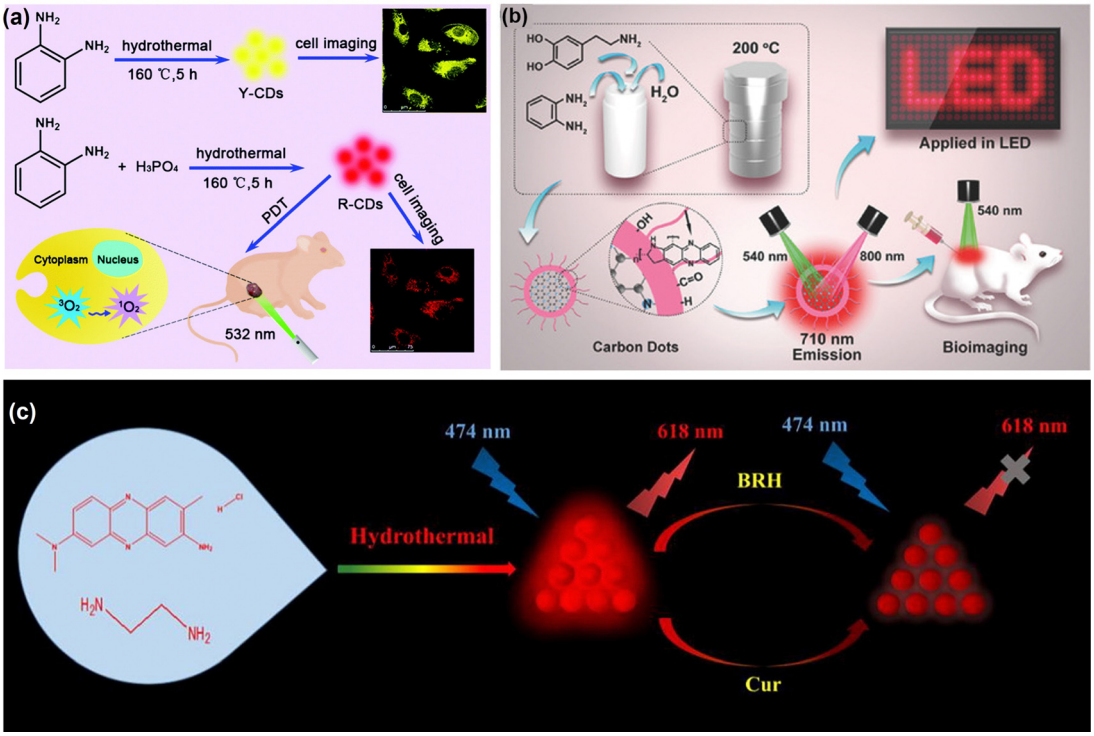

Fig. 3 (a) Syntheses of Y-CDs and R-CDs and their applications in cell imaging and PDT of tumors. Reprinted with permission from ref. 34, Copyright 2019, The Royal Society of Chemistry. (b) Schematic illustration of the preparation and application of NIR-PCNDs. Reprinted with permission from ref. 35, Copyright 2017, Wiley-VCH Verlag GmbH & Co. KGaA, Weinheim. (c) Syntheses of multifunctional R-CDs and label-free fluorescent nanoprobes based on CDs for BRH and Cur detection. Reprinted with permission from ref. 36, Copyright 2021, Elsevier.

which only pure water was used as the electrolyte without any other chemical reagents.[32] The obtained CDs have high crystallinity, excellent water dispersion and remarkable PL properties. Moreover, their PL emission wavelength can extend into the near-infrared (NIR) range upon the excitation of 300–900 nm, which will be promising for biomedical applications.[33] This synthesis method has the advantages of low cost, is easy to control and a high product yield, but the fluorescence quantum yield of the as-prepared CDs is not high. Therefore, this synthetic method needs further refinement for research in the field of R-CDs.

2.2 Bottom-up

2.2.1 Hydrothermal method. The hydrothermal method allows the preparation of CDs by heating specific precursor compounds in an aqueous solution in an autoclave to produce high temperatures and pressure inside the reactor. The process is simple under a mild reaction. As a result, the product obtained is uniform, generally with a high purity level, and the particle size is easy to control. Furthermore, the luminescent properties of the final product can be easily adjusted by changing the experimental conditions, *e.g.*, changing the molar feeding ratio of precursors, solvents, heating time, and temperature.

Zhao *et al.* prepared N and P co-doped R-CDs using a hydrothermal method with *o*-phenylenediamine (*o*-PD) and phosphoric acid as raw materials, which were successfully applied to *in vitro* cell imaging and photodynamic therapy (PDT) studies (Fig. 3a).[34] Lu *et al.* prepared two-photon fluorescent near-infrared emitting polymer carbon nanodots (NIR-PCNDs) using a hydrothermal method with dopamine and *o*-phenylenediamine as raw materials. NIR-PCNDs exhibit intense deep red and NIR luminescence in ethanol solution under white light with non-excitation wavelength-dependent PL.[35] Under 710 nm excitation, the strongest emission of NIR-PCNDs in ethanol solution is concentrated at 665 nm. NIR-PCNDs have specific D–π–A structural domains with large conjugated rigid sp^2-domains responsible for large two-photon absorption cross sections, which can be used *in vivo* bioimaging and red LEDs (Fig. 3b). Meng *et al.* used neutral red and ethylenediamine (EDA) as raw materials to prepare R-CDs using a one-pot hydrothermal method for label-free detection of berberine (BRH) and curcumin (Cur) in a cell imaging process (Fig. 3c).[36]

2.2.2 Solvothermal method. The solvothermal method was developed based on hydrothermal synthesis.[37] The solvent used for the dispersed phase is organic rather than water. Under liquid phase or supercritical conditions, the reactants dispersed in the solution become more active, and the CD products form slowly. The process is relatively simple and easy to control, effectively preventing the volatilization of toxic substances and preparing gas-sensitive precursors in a closed system. However, this method has some disadvantages, such as possible by-products, the low purity level of the final product, and a non-uniform distribution range of size and morphology.

Wang *et al.* prepared R-CDs using the one-step solvothermal method with lignin as a carbon source and *p*-PD as a nitrogen

source.[38] Guan *et al.* prepared dual-emissive N, S co-doped R-CDs using a solvothermal method with *o*-PD and sulfonamide as precursors.[39] Ding *et al.* also used a solvothermal method to produce NIR emission of CDs by heating a formamide solution with lemon juice, which showed a fluorescence quantum yield as high as 31%.[40] The synthesis of R-CDs is closely related to the chosen solvent, which is also beneficial to regulate the optical properties of CDs.

2.2.3 Microwave-assisted method. One method for obtaining CDs is a microwave-assisted method, which uses microwave heating to carbonize organic matter.[41] The experimental conditions for this method are relatively simple and require a shorter time than the hydrothermal/solvothermal synthesis, but the formation of CDs can't be effectively controlled due to the fast reaction rate. Lan *et al.* prepared R-CDs at room temperature and atmospheric pressure by using a household microwave oven-assisted heating of an ammonium citrate tribasic, formamide, and glycerol blend reaction solvent (Fig. 4a).[42] R-CDs in ethanol solution showed an emission peak at 622 nm with a PLQY of 37.4% and exhibited an excitation-independent PL emission spectrum. Therefore, the microwave-assisted method can also be used as a facile and cost-effective synthetic way to modulate the optical properties of R-CDs by optimizing the reaction solvent. In a recent study, Bi and co-workers designed and synthesized new RNA targeting R-CDs (named M-CDs) using the microwave-assisted method by selecting neutral red and levofloxacin as precursors (Fig. 4b).[23] The CDs not only have high RNA selectivity but also bright red fluorescence and a high quantum yield (λ_{max} = 642 nm, Φ_{PL} = 22.83%). Therefore, the microwave-assisted method can also be used as a simple and efficient synthesis method of R-CDs.

2.2.4 Pyrolysis. Pyrolysis is the process of thermal decomposition of organic matter under high temperatures. CDs of different sizes and crystallinities can be prepared by varying pyrolysis conditions such as heating temperature, time and surroundings with/without protecting gas. This pyrolysis method has often been used to prepare fluorescent CDs using natural products (*e.g.*, konjac flour) as raw materials.[43] Although hydrothermal and solvothermal methods commonly synthesize R-CDs, both require high temperature and pressure, complicated post-treatment processes and have relatively low product yields, making them unsuitable for large-scale R-CDs production.[44] In addition, the role of solvents in the synthesis of R-CDs is unclear, leading to ambiguity in the mechanism of R-CD formation, further limiting their usage in the controlled synthesis of CDs. In contrast, the preparation of R-CDs by the

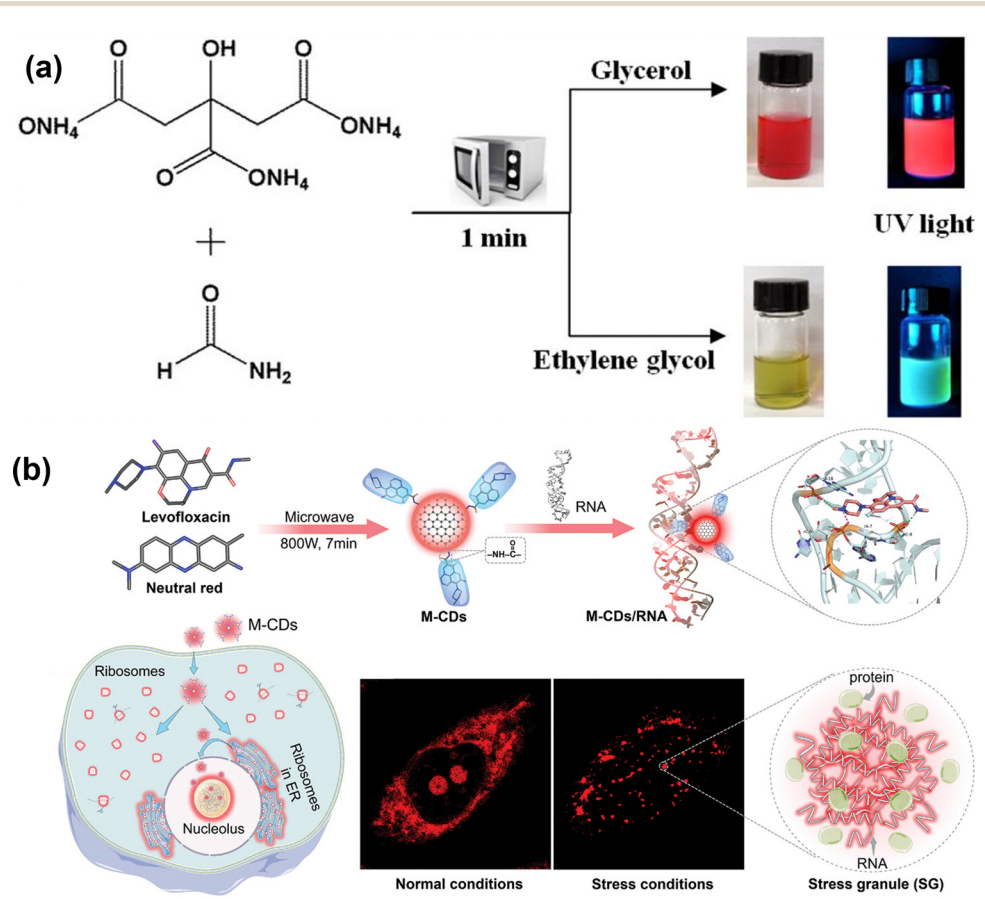

Fig. 4 (a) Synthesis of R-CDs and G-CDs. Reprinted with permission from ref. 42, Copyright 2020, IOP Publishing Ltd. (b) Schematic representation of the M-CDs' synthesis, structure, and RNA binding behaviors of the M-CDs. Schematic illustration of the cellular internalization pathway of M-CDs (ribosomes to nucleolus) and their uses for cellular bulk RNA imaging. Reprinted with permission from ref. 23, Copyright 2023, Wiley-VCH Verlag GmbH & Co. KGaA.

pyrolysis method is solvent-free and requires only heating, avoiding the dangers of high pressure or the inconvenience of solvent post-processing; this allows for large-scale preparation and can be used for the industrial production of R-CDs.[45] Moreover, R-CDs with a narrow emission (λ_{em} = 615 nm, FWHM = 29 nm) were synthesized recently using the pyrolysis method with *p*-PD as a single precursor. This method based on pyrolysis of a single precursor can effectively reduce the type of luminescence centers and ultimately achieve narrow emission of CDs.[46]

At present, the bottom-up method is mainly used to synthesize R-CDs, and its main synthetic mechanism is to make these small molecules dehydrated and carbonized, cross-linked and aggregated to form stable carbon nuclei at high temperatures by using organic small molecules as precursors (*e.g.*, aromatic compounds), and through the reaction conditions of hydrothermal, solvent thermal, and microwave-assisted heating, or further surface modification or passivation, and ultimately obtaining CDs with fluorescent properties.[47] In addition, Xue *et al.* have classified the process of CD formation into three main categories based on the types of precursors of aromatic compounds: amines, phenols, and plastics. Most amines polymerize themselves to form dimers, which then further polymerize.[48] As oxidation deepens, a small fraction of the amine undergoes carbonylation at the amine site, forming the CD structure. For phenolic compounds, most reactions begin with the oxidation of a hydroxyl group to a semiquinone or quinone. Furthermore, unique three-molecule rings are formed through interactions between neighboring molecular groups, such as dehydration. For polycyclic aromatic compounds, the reaction process is more complex, with each reaction precursor having a different formation process.

The main advantage of the bottom-up method for synthesizing of CDs is that it enables the modulation and functionalization of the structure of the CDs, giving them more potential for diverse applications. At the same time, this method can also use sustainable and environmentally friendly raw materials and optimize the synthesis process to achieve the goal of sustainable development. However, this synthetic approach still faces several challenges, such as improving synthetic efficiency, product yield and purity, and further understanding and optimizing the synthetic process.

3. Optical properties

R-CDs have many outstanding optical properties, such as long wavelength absorbance/luminescence, large Stokes' shift, low photobleaching, multi-photon fluorescence and delayed fluorescence.[27] These special properties make R-CDs promising for *in vivo* bioimaging, sensing, photothermal and photodynamic therapy applications.[49]

3.1 Absorbance

R-CDs have three energy absorption processes in the UV-Vis spectrum: the π–π* transition, the n–π* transition, and the surface functional group absorption.[50] Among them, the absorption peaks in the range of 200–280 nm are generally due to the π–π* transitions of the aromatic C=C core. The absorption peaks at 280 nm and above mainly correspond to the n–π* transitions caused by the abundant functional groups possessed by R-CDs, such as C=O, C–N/C=N, or C–S groups.[51] Yang and co-workers synthesized deep-red emissive CDs with a narrow FWHM of 20 nm from biomass precursor taxus leaves (Fig. 5a and c), which exhibited NIR absorption at 600–700 nm and deep-red solid fluorescence under UV excitation (Fig. 5b and d).[20] Furthermore, with the formation of aggregates, the position of the absorption peaks of R-CDs will be shifted, indicating the CDs' π–π stacking effect. With the enhancement of the peak intensity, new absorption bands may appear in the longer wavelength region.[52] The optical properties of R-CDs can be effectively controlled by varying particle size, surface state, and heteroatom doping, of which the choice of reaction solvent and precursor are the two most important factors, and the excitation/emission of the NIR region can be expanded when polycyclic aromatic hydrocarbon and organic dyes are selected as precursors.[53]

3.2 Photoluminescence mechanism

CDs are zero-dimensional carbon nanomaterials with mainly sp^2–C and minorly sp^3–C as the carbon backbone and abundant functional groups/polymer chains on the surface. In recent years, the luminescence mechanism of R-CDs has been a research hotspot, but there are still many controversies due to the diversity of carbon sources, the complicated structure of CDs, and the different synthesis and purification methods.[54] At present, four possible luminescence mechanisms have been applied to R-CDs: carbon core state, surface state, quantum confinement effect, and crosslink enhanced emission effect, as shown in Fig. 6.[55] In most cases, several mechanisms work together to control CD luminescence.

Carbon core luminescence mainly refers to the π–π* transition of sp^2 in the conjugated domain. The precursor has a conjugate structure or can form a conjugate structure during the reaction, and the increase in the sp^2-conjugated domain will lead to a red-shifted emission of CDs. Yang *et al.* used citric acid (CA) as a precursor to synthesize CDs and conducted control experiments using CA-like precursors (tartaric acid, aconitic acid, aspartic acid, malic acid, and maleic acid) to explore the luminescence mechanism of R-CDs.[56] It was demonstrated that the red emission mechanism of CA-like precursors is to adjust the cyclization pattern through the length of carbon chains to form different conjugated rings in the carbon core, with the most prominent emission red-shift of the six-membered ring (244 nm), which also provides a method for the synthesis of high-performance R-CDs from non-aromatic precursors.

On the other hand, most R-CDs have oxygen-containing functional groups such as epoxy, hydroxyl, and carboxyl groups on their surfaces, which introduce defects at the edge of the conjugated structure of CDs, thereby inducing surface state luminescence.[57] Tariq *et al.* rapidly synthesized biomass R-CDs from fresh figs using a microwave-assisted method.[58] The excitation dependent PL of R-CDs shows a slight blue shift of R-CD as

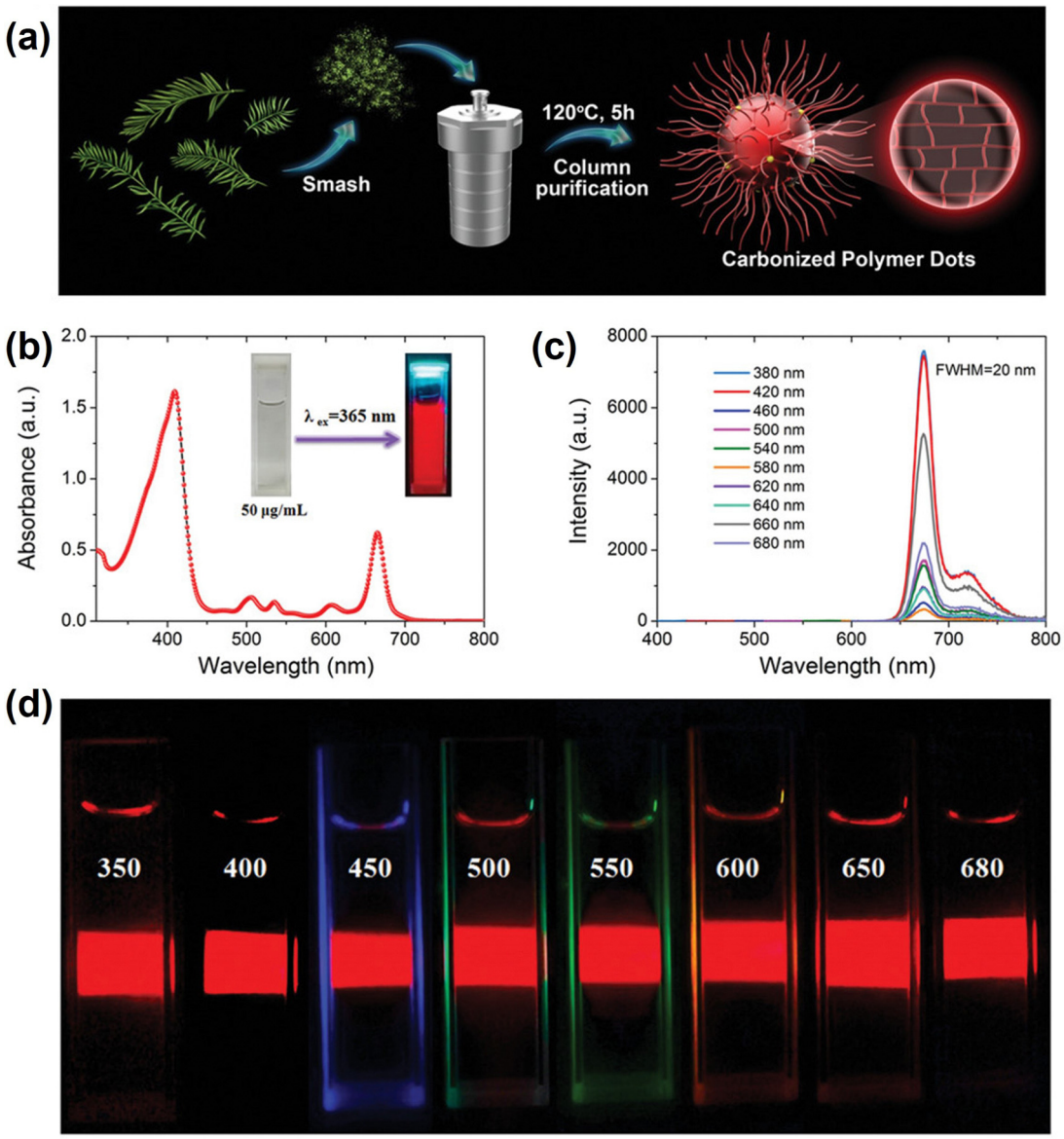

Fig. 5 Synthesis and optical properties of CPDs in acetone solution. (a) A schematic diagram of the synthesis of CPDs. (b) Absorption spectrum, illustration: a photo of CPDs in acetone solution (50 μg mL^{-1}) under sunlight (left) and ultraviolet light (right). (c) PL emission spectra of CPDs at different excitations. (d) CPDs in acetone solution (50 μg mL^{-1}) were excited at the specified wavelength and directly photographed. Reprinted with permission from ref. 20, Copyright 2020, Wiley-VCH Verlag GmbH & Co. KGaA.

the excitation wavelength is continuously increased. Varshney *et al.* used the guava leaf-derived to synthesize biomass R-CDs under microwave irradiation.[59] The renewable resources such as biomass are composed of a variety of organic compounds and are rich in a variety of functional groups. The surface state is determined by the connections between the chemical groups and the surface of the carbon skeleton.[60] Theoretical calculations and experimental results have shown that intrinsic (bandgap-related) transitions strongly depend on the conjugated sp^2 domains and effective conjugation length, which are related to the particle size. The quantum confinement effect is responsible for confining charge carriers within the CDs, leading to discrete energy levels that contribute to photoluminescence. The particle size is varied by adjusting the reaction temperature, reaction time, molarity ratio of the precursor, solvent and heteroatom doping, *etc.*

Therefore, CDs can obtain different sizes of conjugated sp^2 domain and HOMO–LUMO energy levels, resulting in tunable emission. The degree of surface oxidation and the type and number of surface functional groups of CDs are closely related to their surface state fluorescence emission. Regulating the degree of oxidation on the surface of CDs affects the energy levels of their surface states, which leads to the modulation of luminescence emission. In addition, the groups on the surface of CDs can effectively passivate the surface defects of the carbon core, thus forming the surface energy levels and achieving tunable surface state luminescence.[61]

Regarding the bottom-up synthesis of CPDs, Prof. Yang Bai proposed a widely recognized PL mechanism of crosslink

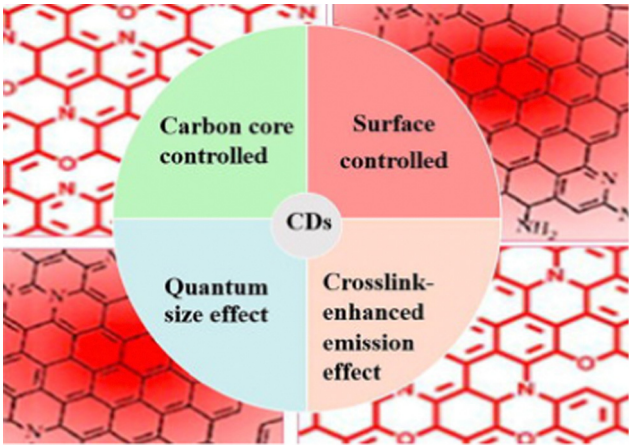

Fig. 6 Major photoluminescence mechanisms of R-CDs. Reprinted with permission from ref. 55, Copyright 2022, Elsevier.

enhanced emission effect (CEE) in as early as 2014, whereby several fluorescent motifs or potential chromophores that do not emit light in the standalone state enhance luminescence by suppressing the vibration and rotation of luminescent centers or forming a new energy hierarchy in response to extensive crosslinking interactions.[62] In 2015, Zhu *et al.* also proposed that the PL of non-conjugated sub-fluorophores such as C═O, C═N, and N═O could be enhanced by chemical crosslinking or physical immobilization of polymer chains.[63] Since then, based on the studies from CDs to CPDs,[2] Yang's group has demonstrated it in polyacrylic acid with an ethylenediamine system[64,65] and the polyacrylamide system[66] that the importance of the CEE effect on the luminescence of CPDs. The CEE effect was further classified into covalent-bond CEE and non-covalent-bond CEE (supramolecular CEE, ionic bond CEE and confined-domain CEE) according to the crosslinking mode.[67] In 2022, Yang and co-workers systematically investigated the confined-domain CEE effect on PL using a well-designed model of CPDs.[68] This series of studies for CEE will contribute to understanding the PL mechanism of CPDs and inspire new ideas for designing synthetic methods to obtain CPDs with many special properties.

In addition, molecular fluorescence and synergistic luminescence also exist. Molecular fluorescence is based on luminescence induced by molecular fluorophores or polymers in CDs. For instance, the luminescent properties of 5,14-dihydroquinoxaline[2,3-*b*] phenazine (DHQP) were investigated and compared with that of CDs to demonstrate that the luminescent center of CDs is a fluorophore in the molecular state.[69] For multi-colored emission of CDs, the fluorescence is usually derived from the synergistic effect of multiple luminescence mechanisms, *e.g.*, the synergistic luminescence of surface and carbon core states can be obtained by controlling the pyrolysis temperature and molar ratio of the reactants. Miao *et al.* synthesized multi-color emissive CDs by controlling the molar ratio of CA to urea in the range of 0–1.0 and the reaction temperature from 140 to 200 °C. The results demonstrated that the enlarged size of sp^2 domains and the increase in surface functional groups changed the PL emission of CDs from green to red.[70]

Solvent and environmental effects are also important considerations that influence the photoluminescent properties of carbon dots. The solvation effect is important for the optical properties of carbon dots. The precursors have better dispersibility in non-polar solvents and are more dehydrated and carbonized, which makes it easier to synthesize R-CDs. Tian *et al.* respectively synthesized fluorescent carbon dots with emission wavelengths ranging from 448–638 nm in water, *glycerol*, and DMF using citric acid and urea as precursors.[71] CDs synthesized in DMF were the most carbonized and had the longest fluorescence emission wavelength. In addition to the effect of solvent polarity on the emission red-shift of carbon dots, the presence of heterogeneous elements such as N, S and O in the solvent also affects the emission peak red shift. A series of CDs with tunable fluorescence emission were prepared by changing the solvent (Fig. 7a and b).[4,72] With the red-shift of CD emission, the N content in the CDs increases and the O content decreases. In addition to organic solvents, acids

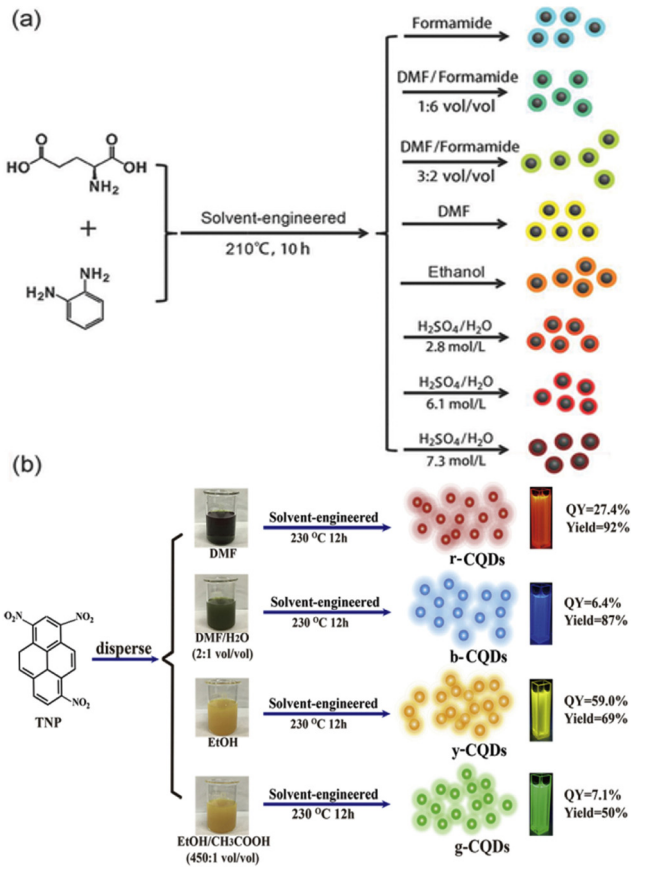

Fig. 7 Solvent effect on carbon spot photoluminescence. (a) Polychromatic fluorescent CDs were synthesized from L-glutamate and *o*-phenylene diamine in different solvents. Reprinted with permission from ref. 4, Copyright 2018, Wiley-VCH Verlag GmbH & Co. KGaA. (b) Polychromatic bandgap fluorescent CDs were prepared using a solvent engineered molecular fusion strategy. Reprinted with permission from ref. 72, Copyright 2018, Elsevier.

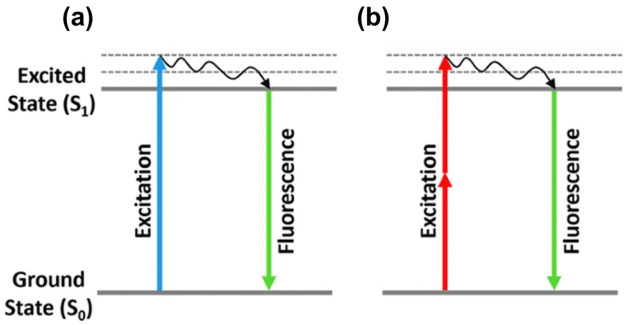

Fig. 8 Energy absorption mechanism of (a) single-photon excitation (blue line), (b) two-photon excitation (red line) and fluorescence emission (green line). Reprinted with permission from ref. 73, Copyright 2021, Springer Nature.

play an important role in achieving the long-wavelength emission of CDs.

Understanding the photoluminescence mechanisms of R-CDs is crucial for controlling their synthesis and encouraging their application with adjustable PL emissions. However, discrepancies in particle configurations have hindered the achievement of a unified process, and the underlying PL emission mechanism is still unknown. Therefore, it is important to advance the development and uses of R-CDs by disclosing their structure and PL mechanism.

3.3 Nonlinear optical properties

In single photon fluorescence, a fluorescent molecule absorbs a photon when irradiated by excited light and is excited from the ground state (S_0) to the excited state (S_1). After internal conversion (IC), it returns from the excited state to the ground state and releases energy in the form of fluorescence emission.[73] Multi-photon fluorescence could be described as a photophysical process observed by some CD structures that absorbs multiple photons simultaneously under laser irradiation from the ground state (S_0) to the singlet excited state (S_1). Unlike single-photon absorption, two-photon absorption involves the simultaneous absorption of two low-energy photons by one electron. The energy of each photon is approximately half of the bandgap, and the wavelength is twice that of the bandgap, causing the valence electrons to be excited to the excited state (Fig. 8).[73]

Compared to single-photon fluorescence imaging, a multi-photon fluorescence profile can improve bio-imaging capabilities and the imaging of complex biological tissues. Particularly, the two-photon fluorescence performance of R-CDs allows for higher resolution bio-imaging of live cells and deep tissue imaging analysis. Liu *et al.* synthesized the R-CDs with a strong NIR absorption/emission using perylene tetracarboxylic dianhydride and urea as precursors through the solvothermal method. After PEI surface modification of the R-CDs, the obtained PEI-CDs exhibited the best two-photon fluorescence performance under the excitation by a 1300 nm femtosecond pulse laser.[21] Fan *et al.* synthesized a new type of nonlinear R-CDs. At 580, 630, 650 and 1064 nm, the nonlinear absorption coefficients of RCDs were 0.65, −3.09, −4.02 and 0.14 cm G W^{-1}, respectively (Fig. 9a–d).[74] Furthermore, the nonlinear absorption changes from saturated absorption to two-photon absorption in the NIR region. Li *et al.* used a 1400 nm femtosecond laser to excite CDs in dimethyl sulfoxide, which produces both two-photon induced NIR emission and three-photon induced red emission from CDs (Fig. 9e–h).[75]

Nitrogen-doped two-photon R-CDs synthesized by Yi *et al.* showed two-photon absorption ranging from 680 to 1000 nm, with a red emission at 605 nm.[76] The quantum yields of the R-CDs under single-photon excitation (546 nm) and two-photon

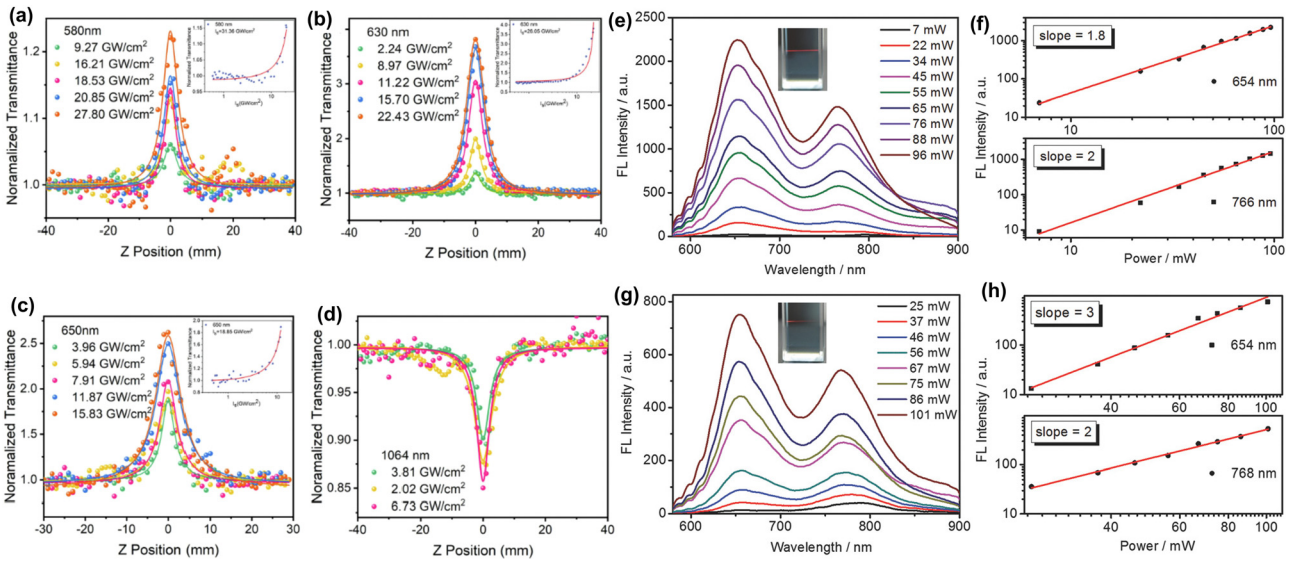

Fig. 9 The R-CDs were characterized by broadband nonlinear optics with excitation at (a) 580 nm, (b) 630 nm, (c) 650 nm, and (d) 1064 nm. Inset: Normalized transmittance as a function of excitation intensity. Reprinted with permission from ref. 74, Copyright 2022 Elsevier. Fluorescence spectra obtained by (e) and (g) multiphoton excitation dependent on the incident intensity, (f) excitation at 1200 nm and (h) emission power dependence at 1400 nm. Reprinted with permission from ref. 75, Copyright 2018, Wiley-VCH Verlag GmbH & Co. KGaA.

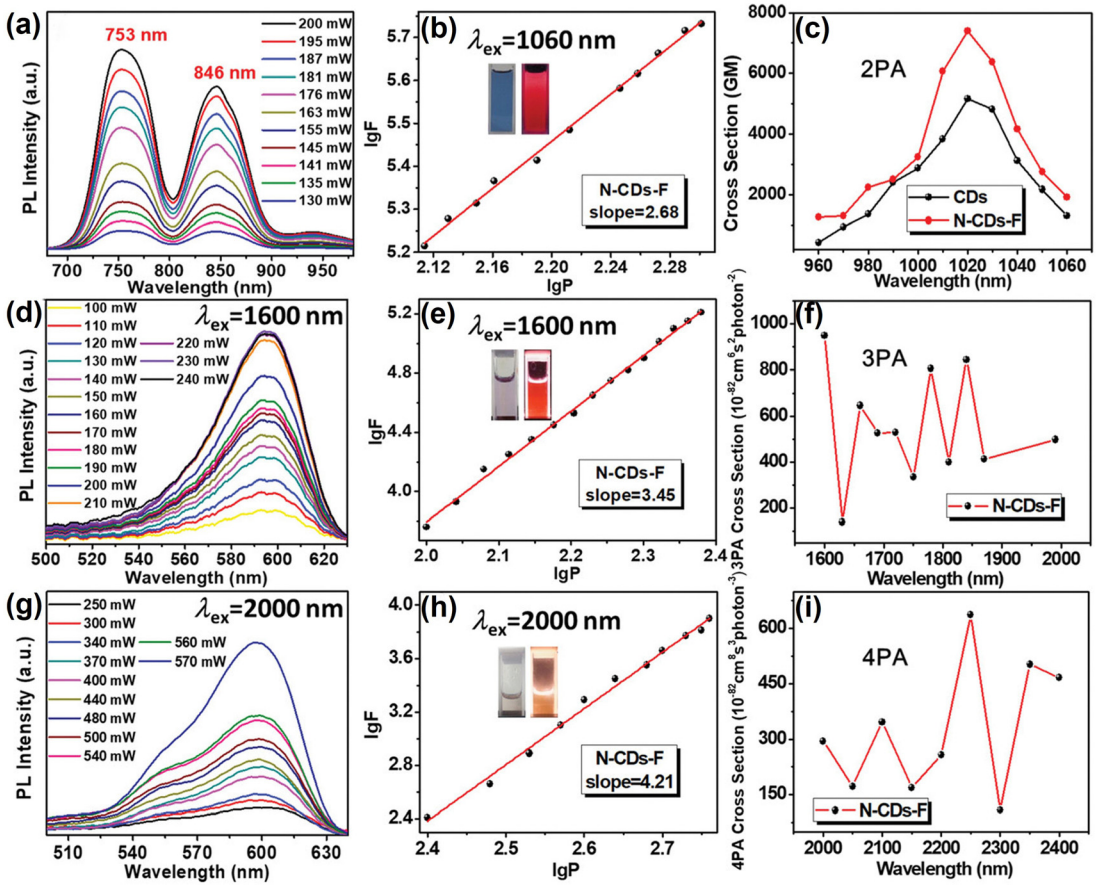

Fig. 10 (a) 2-, (d) 3-, and (g) 4-photo emission PL spectra of N-CDs-F with different laser powers of 1060, 1600, and 2000 nm fs-laser, respectively. Quadratic relationship of N-CDs-F between the integrated fluorescence area and the excitation laser power at (b) 1060 nm, (e) 1600 nm, and (h) 2000 nm, respectively (inset: photograph showing excitation at 1060, 1600, and 2000 nm). (c) 2PA, (f) 3PA, and (i) 4PA action cross sections of CDs and N-CDs-F in DMF. Reprinted with permission from ref. 77, Copyright 2020, Wiley-VCH Verlag GmbH & Co. KGaA.

excitation (700 nm) are 15.1% and 18.2%, respectively. The two-photon excitation property of these R-CDs offers potential applications for bioimaging of living cells and deep tissues. In addition, Jiang *et al.* designed and synthesized fluorine and nitrogen co-doped CDs (N-CDs-F) with a unique electron donor–π–acceptor (D–π–A) configuration, showing excellent two-photon (λ_{ex} = 1060 nm), three-photon (λ_{ex} = 1600 nm), four-photon (λ_{ex} = 2000 nm) and up-conversion fluorescence, while also exhibiting a full range of UV-visible-NIR responses, and it exhibited good fluorescence bio-imaging effects both *in vitro* and *in vivo* (Fig. 10).[77]

3.4 Phosphorescence

Phosphorescence is a photophysical emission process from a triplet excited state (T_1) to the ground state (S_0). This T_1 excited state was generated by an intersystem crossing process (ISC) of excited electrons from S_1 to T_1 as shown in the Jablonski Diagram.[78] CDs, as a room-temperature phosphorescence (RTP) material, have short lifetimes in the S_1 state after light absorption and low phosphorescence efficiency, which can be enhanced by doping with heteroatoms (F, N, B, P, *etc.*) to effectively reduce RTP quenching because of the formation of intramolecular and intermolecular hydrogen bonding.[79–81] The energy gap between the singlet and triplet states can be greatly reduced by introducing electron-withdrawing heteroatoms into the CDs.[82] The formed glassy state can effectively protect the excited triplet state of CDs from non-radiative inactivation to achieve long-life and multi-colored (blue, green, green-yellow and orange) RTP (Fig. 11).[83]

Some CDs can also be embedded in rigid substrates to extend their phosphorescence lifetime and efficiency.[84] Currently, phosphorescent CDs have been widely used in anti-counterfeiting and information encryption,[85–87] but their application in bio-imaging and tumor therapeutic approaches is rare, although red phosphorescent CDs have a lower biological background interference than multi-photon fluorescent imaging. Geng *et al.* combine sonodynamics therapy (SDT) with phosphorescent imaging by designing the structure of CDs cleverly exploiting the p–n junction and narrowing the band gap of CDs to enhance SDT.[88]

3.5 Delayed fluorescence

In the field of light-emitting materials, there are several types of delayed fluorescence (DF) mechanisms that are used, including

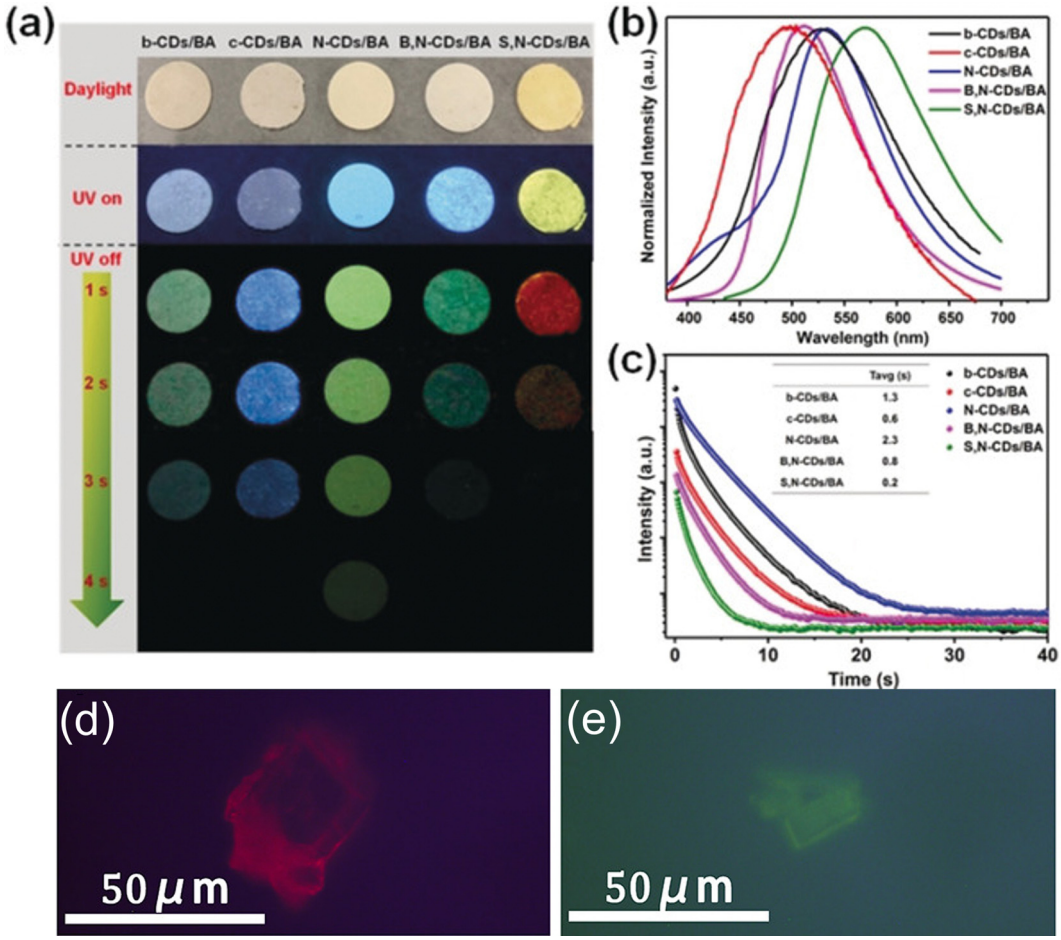

Fig. 11 (a) Photographs of different doped phosphorescence carbon spots before and after turning off 365 nm UV light. (b) Afterglow emission spectra of carbon dot-based RTP materials doped with different heteroatoms excited at 350 nm and (c) afterglow decay curves and lifetimes. Reprinted with permission from ref. 83, Copyright 2019, Wiley-VCH Verlag GmbH & Co. KGaA.

thermally activated delayed fluorescence (TADF), triplet–triplet annihilation (TTA), ''hot excitons'' intersystem crossing (Hot ISC), and defect-induced delayed fluorescence (DIDF). DF materials can convert triplet excitons (T_1) into singlet excitons (S_1) through reverse intersystem crossing (RISC), which is facilitated by a reduction in the spatial overlap between the HOMO and LUMO energy levels (Fig. 12).[89] These materials offer the potential to combine the low cost of fluorescent materials with the high efficiency of RTP materials. However, due to luminescence quenching, generating red DF by combining CDs with TADF materials directly can be difficult.

TADF is a process that enables a material to harness and utilize triplet excitons, which are crucial for improving the efficiency of organic light-emitting diodes (OLEDs). The combination of R-CDs and TADF properties can be used in organic optoelectronics, particularly in OLEDs.[90] R-CDs can efficiently generate and harvest triplet excitons under electrical excitation, allowing them to undergo a TADF process, converting them into singlet excitons, and emitting red light with a delayed fluorescence.[91] These TADF materials can be incorporated into OLEDs, leading to lower power consumption and longer device lifetimes, making them more energy-efficient and durable. One recent study by Lou *et al.* synthesized R-CDs using cucumber skin as a precursor through solvothermal synthesis and incorporated them into a rigid matrix.[92] The RTP-assisted electron transfer strategy was used to form high-efficiency TADF in the R-CDs. The rigid crystal grid enhances the RISC between the S_1 and the T_1 state by enhancing the spin–orbit coupling while effectively suppressing the non-radiative transition efficiency and promoting the generation of TADF phenomenon.

4. Biomedical applications

R-CDs are widely used in biomedical applications due to their excellent water solubility, extremely low toxicity, extended wavelength absorption/emission, deep tissue penetration and excellent biocompatibility. R-CDs have excellent optical properties and produce high contrast *in vivo*, which can be used for *in vivo* imaging. By interacting with biological tissues, R-CDs can provide high-resolution images that help to observe and diagnose a patients' biological tissue status. Moreover, R-CDs have a high efficiency of photothermal conversion when irradiated using an infrared laser, and the quickly increasing

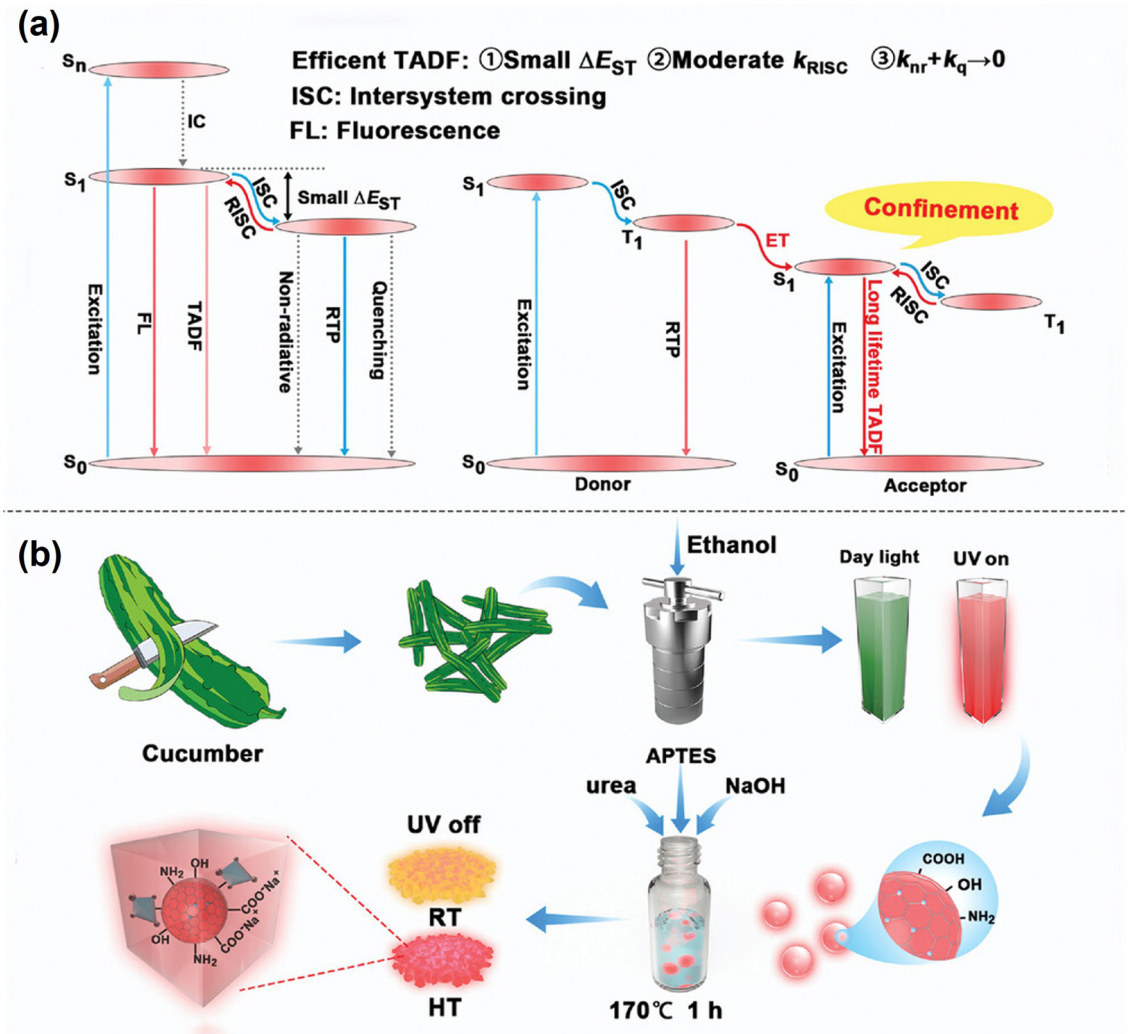

Fig. 12 (a) Left: TADF mechanism with small ΔE_{ST}, moderate k_{RISC} and slow k_{nr} and k_q. Right: The proposed mechanism for achieving TADF with a long lifetime. The persistent excited energy is transferred from the RTP emission center as the donor to the acceptor, thus prolonging the lifetime of TADF. ΔE_{ST} is the energy gap between S_1 and T_1; k_{RISC} is the rate of RISC; k_{nr} represents the non-radiative transitions from the T_1; k_q is the rate constant of triplet-exciton quenching through interactions with surrounding molecules; IC is the internal conversion. (b) Schematic of the design strategy and synthesis of the uCDs@SiO_2/NaOH. RT is room temperature; HT is high temperature. Reprinted with permission from ref. 89, Copyright 2023, Wiley-VCH Verlag GmbH & Co. KGaA.

temperature can be used to kill cancer cells or treat other diseases to achieve therapeutic effects.[93]

4.1 Biomedical imaging

The materials currently used for bioimaging are mainly organic dyes and conventional quantum dots. Compared to these two materials, CDs have distinct advantages when applied to bioimaging, and their excellent photostability and good biocompatibility greatly enhance their potential for biomedical applications.[50] CDs with red/NIR emission properties can be used for bioimaging with excellent fluorescence tunability, good biocompatibility and deep tissue penetration to achieve good light penetration depth and minimize photodamage and autofluorescence interference to biological tissues. They can be widely used in the biomedical field through an image-guided approach.[94]

R-CDs are a type of carbon-based nanoparticle that exhibit unique optical properties. They can give off fluorescence in the red or NIR spectral range, which makes them particularly useful in different imaging applications like Super Resolution Microscopy (SRM).[95] R-CDs as a fluorescent probe can be functionalized with fluorescent labels to identify specific biological structures or molecules, thus improving imaging contrast and reducing background noise. They can also be engineered to emit light at different wavelengths, enabling multi-color imaging for a more comprehensive understanding of complex biological systems.[96] Compared to traditional organic dyes, R-CDs offer improved photostability and reduced phototoxicity, allowing for longer imaging durations without affecting cell viability.[97] Precise localization of individual fluorescent labels is essential for achieving super-resolution in SRM techniques, and R-CDs can provide nanometer-scale spatial

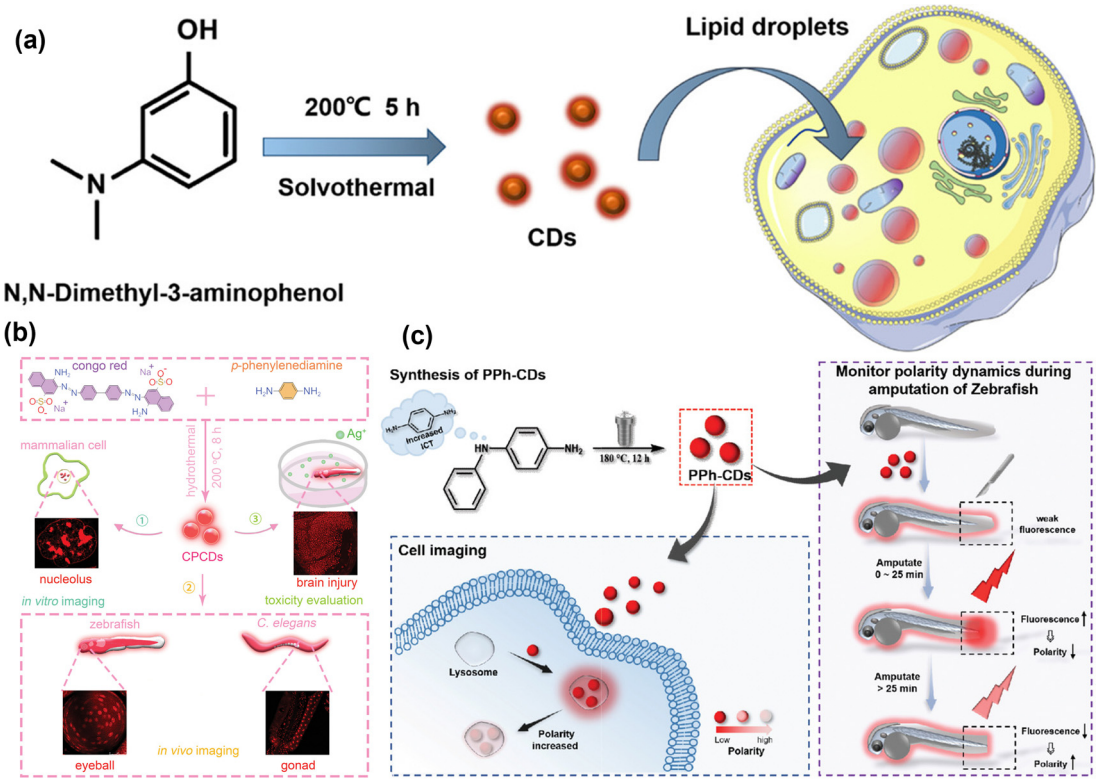

Fig. 13 (a) Synthesis and spectroscopic studies for CDs. Reprinted with permission from ref. 98, Copyright 2022, American Chemical Society. (b) Schematic illustration of the fabrication of CPCDs and their use for *in vitro*/*in vivo* nucleolus imaging and toxicity evaluation. Reprinted with permission from ref. 100, Copyright 2023, Wiley-VCH Verlag GmbH & Co. KGaA. (c) Rational design of the polarity-sensitive PPh-CDs and the use of the CDs in monitoring polarity changes during amputation of zebrafish. Reprinted with permission from ref. 103, Copyright 2021, Wiley-VCH Verlag GmbH & Co. KGaA.

information for improved resolution. Biocompatibility is also a critical consideration for biological imaging applications, and researchers are working on developing R-CDs that are compatible with living cells and biological tissues, which is crucial for SRM studies under physiological conditions.

4.1.1 Organelle-targeted imaging. Organelle-targeted imaging is a technique that enables quantitative imaging of organelles using special fluorescent probes or markers. These probes or markers can selectively bind to different organelles and emit fluorescence or absorb specific wavelengths of light that can be observed with a microscope during imaging. This technique allows further study of cell structure and function and the distribution and interaction of specific molecules in different organelles.

R-CDs can be surface-modified to enable targeted imaging of organelles. Targeting molecules (*e.g.*, drugs, antibodies, *etc.*) to specific organelles can also be covalently bound to R-CDs' surface to enable targeted imaging of specific organelles. In addition, it is also possible to selectively bind to different organelles using the positively/negatively charged or hydrophilic/hydrophobic properties of the R-CDs surface. Lipid droplets (LDs) are dynamic organelles that play a crucial role in regulating neutral lipid storage and energy homeostasis. Jing *et al.* synthesized R-CDs by solvothermal treatment of 3-dimethylaminophenol, and the as-synthesized R-CDs showed deep-red emission with strong LDs targeting (Fig. 13a) and excellent imaging tracer properties.[98] In addition, the nucleus is the control center of the cell, involved in many important physiological activities and is an ideal target for assessing the state of the cell or organism. Wu's group added various metal ions during the hydrothermal treatment of *p*-PD,[99] forming fluorescent CDs with emission wavelengths up to 700 nm. *p*-PD and nickel ions (Ni^{2+}) were used as raw materials to prepare Ni-*p*-PCDs with high fluorescence quantum yields, which benefit from their polarity-sensitive and selective RNA-responsive fluorescence properties. Ni-*p*-PCDs can exhibit highly enhanced fluorescence emission upon entering the hydrophobic intracellular environment, especially in the nucleolus. Thus Ni-*p*-PCDs can successfully stain living mammalian cells. Afterward, Wu and co-workers synthesized bright R-CDs with polarity-dependent fluorescence emission (termed CPCDs) using a one-step hydrothermal method with Congo Red and *p*-PD as precursors (Fig. 13b).[100] The CPCDs enabled wash-free, real-time, long-term, high-quality nucleolus imaging of live cells *in vivo* in two common models: zebrafish and Caenorhabditis elegans. The strategy used by CPCDs to visualize the structure and dynamic behavior of live zebrafish and Caenorhabditis elegans demonstrates the important role of R-CDs in nucleus-targeted imaging.

Lysosomes are spherical, single-membrane organelles in eukaryotic cells that contain a variety of hydrolytic enzymes and are the cell's waste disposal sites, responsible for breaking

down a variety of endogenous and exogenous macromolecules, as well as other cellular organelles.[101] They are essential for a variety of physiological processes including protein degradation, autophagy and endocytosis. Lysosomal dysfunction has been associated with cancer, neurodegenerative diseases and cardiovascular diseases. Selective imaging of lysosomes by R-CDs can be achieved by surface modification of molecules or compounds targeting lysosomes.[102] For example, antibodies or small molecules that find lysosomes can be modified on the R-CDs' surface to enable lysosome imaging using immunofluorescent staining (Fig. 13c).[103] In addition, targeted imaging of lysosomes can also be achieved by surface modification of peptides or proteins with lysosomal location sequences, allowing the R-CDs to bind to the lysosomal membrane. Deng *et al.* synthesized lysosomal targeting probes of boron (B) and nitrogen (N) co-doped CQDs (B/N-CQDs) through a novel and green solid-state reaction, which exhibited a red emission at 618 nm, high quantum yield (28%) and excellent photostability.[22] The boron dopant in the structure of these B/N-CQDs achieves lysosome-specific targeting through borate esterification of the boronic acid moiety in the sample with diol structures in glycoproteins. This can be applied as a powerful tool for tracking apoptosis or necrosis. In the future, further optimization of surface modification and synthesis methods of R-CDs will further promote their wide applications in targeted imaging of lysosomes and other cellular organelles.

Moreover, targeting mitochondria with R-CDs can be achieved by rational surface modification. For example, a peptide or antibody targeting mitochondria can be covalently bound through CD surface modification to enable targeted imaging of mitochondria.[104] Alternatively, mitochondria-targeted imaging can also be achieved by attaching R-CDs with small molecules or compounds that selectively bind to the membrane surface of mitochondria through electrostatic or hydrophilic/hydrophobic properties of the CDs.[105,106] This method has excellent selectivity and sensitivity and can be used to study cellular mitochondrial function and dysfunction processes.

In addition to targeting the above organelles for imaging, R-CDs can target other organelles such as the endoplasmic reticulum and Golgi apparatus through surface modifications (Table 1). In these imaging applications, the surface modification of R-CDs is a crucial optimization factor, allowing for the targeted imaging of different organelles by selectively binding specific molecules or compounds.[112] Designing and synthesizing organelle-targeted R-CDs that excite independent fluorescence emission could further enable high-resolution cell imaging and *in vivo* tracking. By continuously optimizing CDs and selecting appropriate targeting ligands, multifunctional CDs can be designed and synthesized, ultimately achieving higher imaging accuracy and sensitivity.[8] Overall, R-CD targeted imaging has great potential in the biomedical field. Despite the potential of R-CD-targeted molecular imaging, its practical application still has huge challenges and difficulties. For example, there is a need to optimize the surface modification of R-CDs further to improve their targeting specificity and imaging accuracy and to improve their stability in reducing their harmful side effects in living organisms.

4.1.2 Dynamic imaging. Dynamic imaging is a technique used to observe and record the activity of cells or tissues. It typically involves using a microscope and fluorescent dyes to label different structures or molecules within cells and capturing a series of images to record the changes that occur over a specific period. Dynamic imaging of cells provides valuable insights into the details and mechanisms of cellular behavior and has found a wide range of applications in biology, medicine, and bioengineering.[113] CDs, as highly efficient photosensitizers with nanoscale dimensions, can not only enter cells but also label organelles or intracellular substances, delivering excellent cell imaging results. R-CD dynamic imaging uses the unique fluorescence properties of R-CDs to enable real-time monitoring and imaging of cells or tissues in dynamic processes under appropriate conditions. More importantly, because of their photostability and biocompatibility, R-CDs can be imaged for long periods in living organisms without significant toxicity or harm to the organisms.

Wang *et al.* developed far-red to NIR-emissive CDs with intrinsic LD targeting capabilities by carefully substituting *p*-PD with 4-piperidinylaniline to increase the hydrophobicity of the precursor.[111] The obtained PA-CDs can be selectively enriched in LDs due to their lipophilic properties. As shown in Fig. 14a, the nucleus, mitochondria and LDs are visualized in the blue, green and red channels, respectively. Most of the LDs show no contact with the mitochondria. As investigated, the ability of PA-CDs to sense LDs dynamics in real-time by pseudocolor was assigned to LDs at 0, 30, 60 and 90 s, and merged images of two adjacent times showed the movement of LDs relative to the previous time point (Fig. 14b). The dynamic behavior of LDs in the observed region (dissociation, migration

Table 1 Summary of R-CD applications in different biological imaging

Modes of imaging	Names of CDs	Synthesis methods	Sizes (nm)	Cell models	Specific targeting sites	Pearson's coefficients	Ref.
Organelle-targeted imaging	Red CDs	Hydrothermal	2.60 ± 0.68	HeLa	Endoplasmic reticulum	0.9	107
	PPh-CDs	Solvothermal	3.2	HeLa	Lysosome	0.87	103
	CDs	Solvothermal	6	HepG2	Lipid droplet	0.9	98
	RCDs	Solvothermal	4	4T1	Mitochondrion	0.96	108
	GTCDs	Solvothermal	3.36 ± 0.98	HeLa	Golgi apparatus	0.92	109
	CPCDs	Hydrothermal	5.6 ± 4.2	A549	Nucleolus	0.91	100
Targeted molecular imaging	M-CDs	Microwave-assisted	1.6	HepG2	RNA	0.92	23
	C-dots	Microwave-assisted	2.8 ± 0.8	HeLa	DNA	>0.85	110
Dynamic tracking imaging	PA CDs	Solvothermal	1.2–3.0	HeLa	Lipid droplet	0.91	111

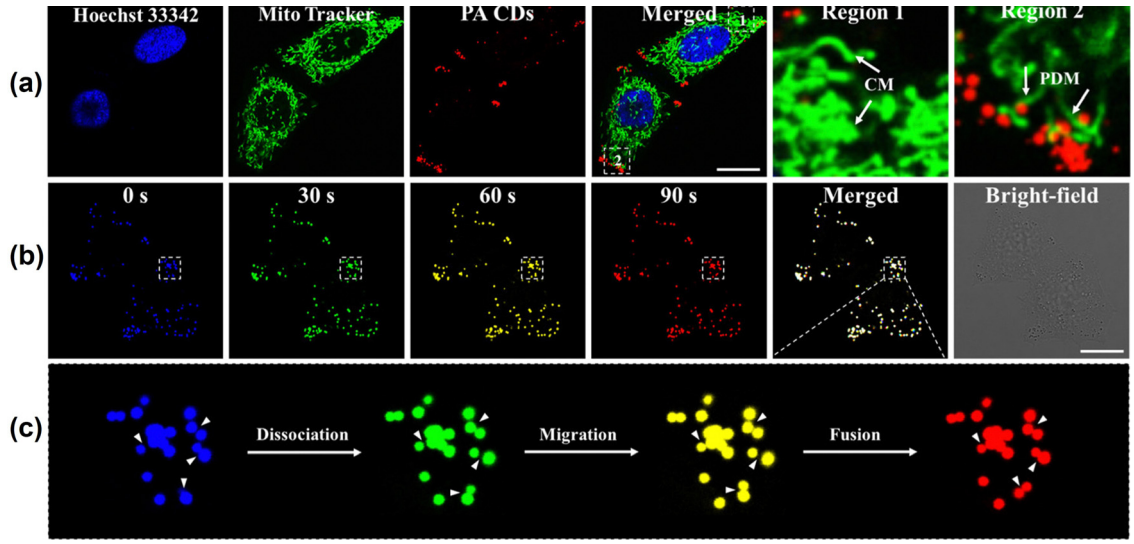

Fig. 14 (a) Confocal imaging of HeLa cells stained with Hoechst 33342 (1 μL) for the nucleus, Mito Tracker Deep Red FM (500 nM) for mitochondria, and PA-CDs (10 μg mL^{-1}) for LDs. (b) Real-time tracking of LDs movement by PA-CDs: the movement of LDs at 0, 30, 60, and 90 s is illustrated by four different pseudo-colors and the merged image of all the images. (c) The enlarged image comes from the square area marked in (b). Scale bar: 20 μm. Reprinted with permission from ref. 111 Copyright 2021, American Chemical Society.

and fusion) was visible within 30 s (Fig. 14c). This highly dynamic behavior accelerated the metabolism of LDs for cell proliferation, and repeated laser irradiation during imaging did not significantly affect the brightness of the CDs. Thus, the R-CDs can be used for real-time and long-term imaging of LDs' dynamic behavior and spatial distribution, as well as investigating the interaction between LDs and mitochondria.

When cells are exposed to stress conditions, high concentrations of RNA and proteins will aggregate together to form membrane-less organelles called stress granules (SGs). Inspired by the ability to label large amounts of RNA in living cells, Jiang *et al.* designed and synthesized M-CDs that can specifically target RNA (Fig. 15) and rapidly internalize into cells.[23] Live HepG2 cells were stained with the M-CDs and then treated with sodium arsenite (SA, $NaAsO_2$, a common stress-inducing compound). As shown in Fig. 10a, the M-CDs staining pattern showed time-dependent recombination with RNA being able to repolymerize after SA treatment. Meanwhile, live cell workstation monitoring by several cancer cell lines (Fig. 15b) revealed that the localization of nucleolar RNA changed over time and the fluorescence in the nucleolus gradually faded, suggesting that RNA synthesis and processing are affected by oxidative stress and that M-CDs have the versatility to assemble SGs when imaged intracellularly.

4.1.3 Multimodal imaging. R-CDs are widely used in multimodal imaging because of their excellent chemical stability, biocompatibility, photostability and deep tissue penetration. In particular, it is preferrable for R-CDs to be used in fluorescence imaging and photoacoustic imaging (PA) by combining fluorescence detection with ultrasound detection based on photoacoustic effects to enable imaging beyond the light diffusion limit, providing deeper tissue imaging penetration and higher spatial resolution. Ge *et al.* used a polythiophene derivative (PT2) as a carbon source to prepare CDs with a broad absorption band at 400–800 nm and a red emission at 640 nm.[114] It is the first time that R-CDs have been used for cancer diagnosis using PA and cancer treatment using thermal therapy in living mice. When transition metal-doped CDs such as Fe, Ni, Co, Mn, and Gd are used, non-invasive imaging of tissue structure or metabolic features can be achieved by magnetic resonance (MR) imaging. Recently, Jiao *et al.* synthesized Gd-doped CDs (Gd-CDs) using a one-step solvothermal method for fluorescence/MR imaging-guided photothermal cancer therapy.[115] The aptamer AS1411 was used to form AS1411-Gd-CDs by coupling on the surface of the synthesized Gd-CDs to improve tumor targeting. Tumor-specific fluorescence/MR dual-modality imaging was successfully achieved with AS1411-Gd-CDs under both *in vivo* and *in vitro* conditions. In addition, AS1411-Gd-CDs exhibited significant tumor inhibition under fluorescence/MR imaging guidance with apparent photothermal effects.

The liposomal CDs nanohybrid system (PEG-RLS/Fe@CDs) prepared by Luo *et al.* consists of iron-doped carbon dots (Fe@CDs) derived from iron(II) phthalocyanine and an amphiphilic lipopeptide assembly (DSPE-mPEG2000/RLS) (Fig. 16).[116] Due to its excellent photothermal conversion (g = 63.4%), the gene transfection efficiency was increased by 3.5-fold in 4T1 tumor cells and by 2-fold in animal models. Fe@CDs in nanohybrids can be used as a four-modal contrast agent for fluorescence/PA/photothermal and MR imaging, showing up to three orders of magnitude enhancement of the photoacoustic signal. These reveal CDs as a promising candidate platform for improved gene therapy through transfection enhancement, real-time tracking and tumor synergistic destruction for further widespread biomedical applications.

Furthermore, Tian *et al.* prepared nickel and nitrogen co-doped CDs (Ni-CDs) using a simple one-pot hydrothermal method for imaging-guided phototherapy (PTT) in the NIR-II

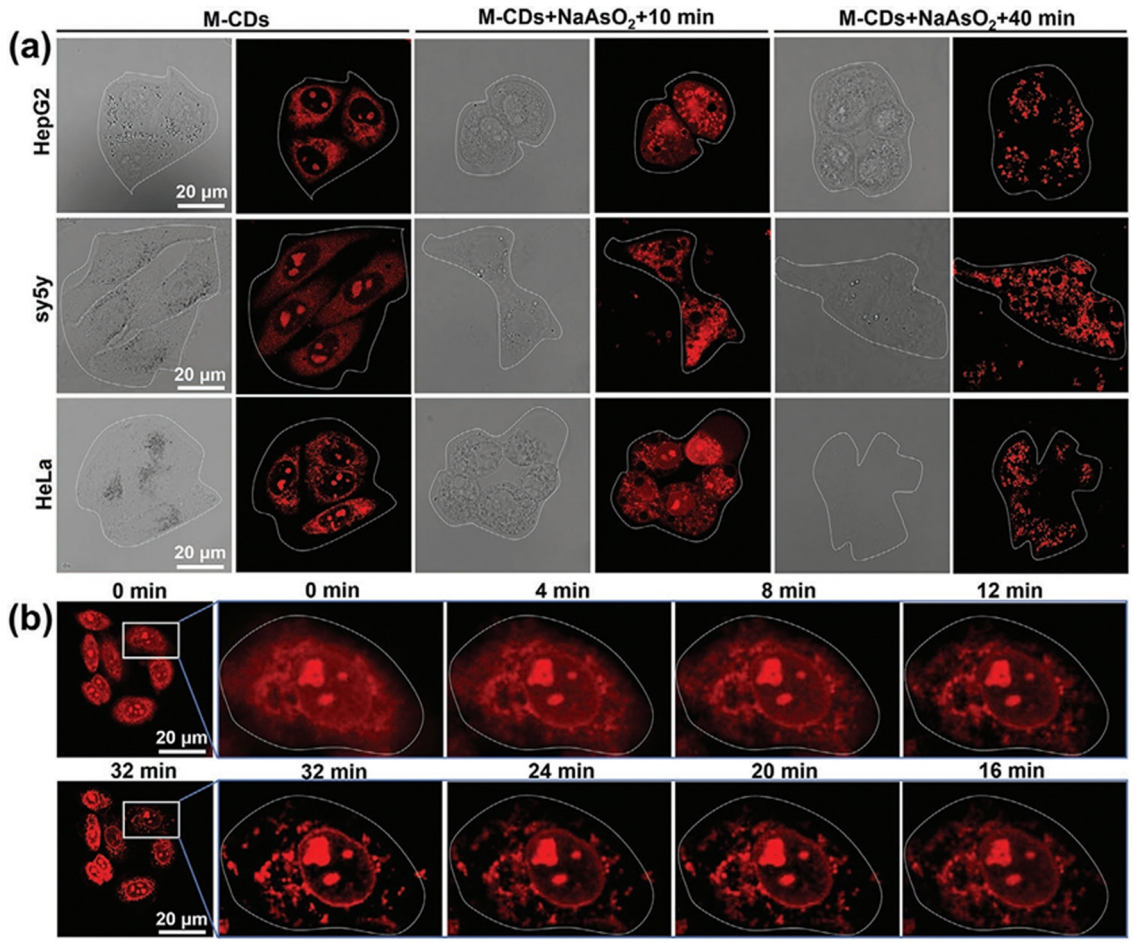

Fig. 15 (a) Confocal images of HepG2 cells, sy5y cells and HeLa cells exposed to M-CDs, M-CDs + $NaAsO_2$ + 10 min and M-CDs + $NaAsO_2$ + 40 min (λ_{ex} = 561 nm). (b) Time-lapse imaging stress granule assembly and early dynamics in HepG2 cells when adding M-CDs during $NaAsO_2$ stress using a 63× objective (λ_{ex} = 561 nm). Reprinted with permission from ref. 23 Copyright 2023, Wiley-VCH Verlag GmbH & Co. KGaA.

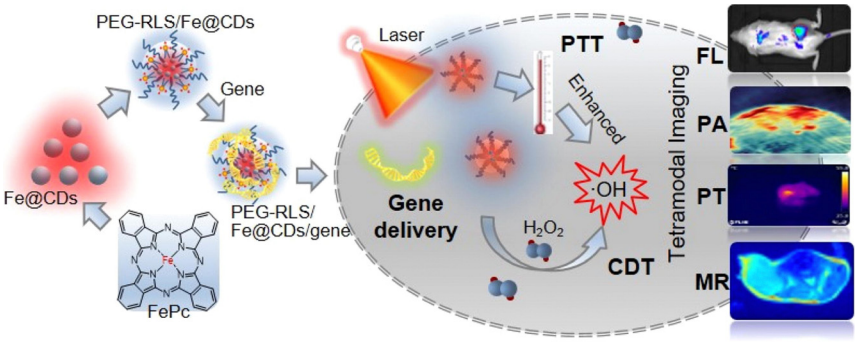

Fig. 16 Schematic representation of iron-doped CDs as a therapeutic agent for PTT, enabling gene delivery and multimodal (MR/PA/PT/FI) imaging-guided PTT/chemo-kinetic therapy. Reprinted with permission from ref. 116. Copyright 2021 Elsevier.

window.[117] Ni-CDs exhibit significant absorption in the NIR-II region, have a remarkable photothermal conversion efficiency of up to 76.1% (1064 nm), and have excellent photostability and biocompatibility. In addition, Ni-CDs can be used as photothermal, PA and MR imaging contrast agents due to their outstanding photothermal effect and innate paramagnetic properties. Ni-CDs can be cleared from the body *via* the renal filtration pathway, thus minimizing their long-term biotoxicity, and this work provides a simple and feasible approach for the development of photothermal agents with significant photothermal conversion efficiency in the NIR-II region, providing good biosafety for multimodal imaging-guided tumor PTT.

Multiple imaging techniques coupled with relevant therapeutic means, R-CDs are expected to develop into a multifunctional nano-platform for multi-modal diagnostic and therapeutic integration that can realize comprehensive and multi-dimensional imaging of biological samples, thus providing a more comprehensive understanding of the internal structure and function of biological samples.

4.2 Photodynamic therapy

PDT is a new method for treating tumors with photosensitizing drugs and laser activation. PDT refers to the oxidative action against cancer cells or tissues through controlled production of reactive oxygen species (ROS) by photosensitizer molecules under appropriate photoexcitation. The advantage of PDT over conventional therapies is that it can precisely and effectively treat tumors and be used as a coadjutant therapy with minimal side effects. In addition, because NIR fluorescent CDs have good water solubility and high biocompatibility, they can penetrate deep into the target tissues for further light activation and work as a photosensitizer used in tumor treatment by PDT.[55]

CDs as a photosensitizer work by the two classic photosensitization mechanisms defined as types I and II. Type I refers to the photon-induced generation of electron–hole pairs in the excited state of the molecules. Regarding CDs, the type I photosensitization process refers to the generation of electron–hole pairs in the excited state of the CDs under laser irradiation, and electron–hole pairs produce oxygen radicals through electron transfer with surrounding oxygen molecules present in a biological medium, such as hydroxyl radicals ($^{\bullet}OH$) and superoxide anion radicals ($^{\bullet}O_2^-$).[118] The Type II reaction, also known as the singlet oxygen ($^1O_2$) mechanism, where the photosensitizer CDs could, after photoactivation, produce a triplet excited state (T1) can simultaneously transfer energy to the triplet oxygen molecules leading to the production of the excited $^1O_2$, which immediately reacts with neighboring biomolecules to cause cell destruction and damage, through a classical cell death mechanism such as necrosis, apoptosis or autophagy.[77] An ideal photosensitizer should have low toxicity, high generation of $^1O_2$ or other ROS, and a strong absorption in the longer wavelengths range (such as 600–1000 nm).[119]

Using lysine, *o*-PD and sulfuric acid as raw materials, Zhao's group prepared S and N co-doped CDs (S, N-CDs) with long wavelength absorption through a classical hydrothermal synthesis.[120] The S, N-CDs showed a therapeutic efficiency higher than that observed by N-doped CDs and the CDs without doping. Electron spin resonance (ESR) experiments with 1,3-diphenylisobenzofuran (DPBF), a well-known $^1O_2$ rapping, showed that CDs could efficiently produce $^1O_2$ in cells under a 660 nm laser irradiation. The CDs synthesized by Li *et al.* exhibit tunable enzyme mimic activity under NIR emission and have an excellent surface-enhanced Raman scattering (SERS) performance.[121] The CDs were used to monitor NIR emission-induced peroxidase-like catalytic processes in tumors by using the SERS strategy. In addition, glutathione depletion occurred through cascade catalytic reactions, thereby increasing intratumor oxidative stress based on NIR photo-induced enhanced peroxidase and glutathione oxidase-like activity, amplifying ROS damage. These NIR-absorptive CDs are potentially beneficial to be used in fast PDT treatment promoted by photothermal activity within 3 minutes of treatment, leading to the apoptosis of cancer cells. More recently, Bi and co-workers found that a certain kind of RNA-targeting R-CDs showed a superior $^1O_2$ generation yield (54.33%) in response to intracellular RNA binding under visible LED light irradiation, which could be developed as a new type of photosensitizer for achieving pyroptotic cancer cell death in PDT.[122]

To allow readers to understand more about the advantages of R-CDs used for PDT, we have summarized the related

Table 2 Summary of R-CD parameters used for tumor photodynamic therapy

Name of CDs	Excitation wavelength	Emission wavelength	QY	Light wavelength	Light power	Types of ROS	ROS QY	PDT effect	Ref.
R-CDs	560 nm	622 nm	15%	532 nm	100 mW cm^{-2}	$^1O_2$	—	A549 cell viability decreased to 18% after treatment	34
p-RCDs	488 nm	680 nm	—	635 nm	100 mW cm^{-2}	$O_2^{\bullet-}$, $^1O_2$	42%	4T1 cell viability decreased to 48% after treatment	108
MMCDs	520–560 nm	642 nm	7.11%	400–500 nm	100 mW cm^{-2}	$^1O_2$, NO	—	HepG2 cell viability decreased to 20% after treatment and the tumor growth was significantly inhibited	122
C-dots	552 nm	560–590 nm	42.7%	400–700 nm	150 mW cm^{-2}	ROS	4.8%	The 4T1 cell tumor volume decreased significantly after treatment	118
S,N-CDs	600 nm	630 nm	12.4%	660 nm	0.6 W cm^{-2}	$^1O_2$	27%	HeLa cell viability was less than 10% after treatment	120
CDs-10	540 nm	630 nm	26.06%	400–500 nm	15 mW cm^{-2}	$^1O_2$	38.85%	HepG2 cell viability decreased to 10% after treatment	123
Cu,N-CDs	—	726 nm	6.0%	808 nm	1 W cm^{-2}	$^1O_2$	—	B16 cell viability decreased to 20% after treatment	124
OCDs	900 nm	580 nm	10.3%	white light	10 mW cm^{-2}	$^{\bullet}OH$	—	The 4T1 cell tumor volume decreased significantly after treatment	125
RCNDs	485 nm	500–800 nm	0.4%	660 nm	100 mW cm^{-2}	$^1O_2$	52%	HeLa cell viability decreased to 30% after treatment	126
N,S-CDs	—	625 nm	2.5%	white light irradiation	14 mW cm^{-2}	$^1O_2$	8%	HeLa cell viability decreased to 15% after treatment	127
GQDs	488 nm	680 nm	1.3%	400–800 nm	80 mW cm^{-2}	$^1O_2$	75%	HeLa cell viability decreased to 20% after treatment	128
TP-CDs	546 nm	605 nm	15.1%	638 nm	1 W cm^{-2}	$^1O_2$	—	HeLa cell viability decreased to 22% after treatment	76

parameters such as the species of R-CDs, their excitation/emission wavelengths, the generated ROS types and their respective generation yields, the wavelength and power of the light that used for PDT as well as the PDT effect on tumor cells or tumors, as shown in Table 2. It is noteworthy that a higher PDT effect on tumors can be obtained by choosing an appropriate incident wavelength and the power of the light to irradiate the R-CDs.

4.3 Photothermal therapy

PTT is the conversion of light energy into heat by photosensitizers, which uses excessive heat to cause irreversible damage to cancer cells and destroys them.[129] Traditional chemotherapeutic drugs can be systemically toxic to the body while treating tumors. In contrast to PDT, PTT does not require the involvement of oxygen and is therefore not limited by the lack of oxygen in the tumor. PTT can perform the treatment at the tumor site by controlling the laser irradiation area, thus achieving tumor-specific treatment and avoiding damage to normal tissues, and CDs with PTT effects have broad application prospects in tumor treatment.[130] In addition, CDs with specific and targeted therapeutic functions toward tumors and their microenvironment are also attracting attention as research progresses.

Qu's group prepared CDs with a photothermal conversion efficiency of up to 59% using the solvothermal method, and an emission profile with a NIR fluorescence peak at 720 nm (λ_{ex} = 655 nm).[131] The excellent photothermal properties of CDs indicate that they are effective photothermal agents for PA imaging as well as PTT applications.[132] In the literature, the photothermal conversion efficiency of R-CDs was at the highest level among carbon-based nanomaterials and comparable to other inorganic nanoparticles that have been studied.[133–135] Zhao *et al.* prepared CDs showing emission in the NIR-I region and an extended absorption peak in the NIR-II region using solvent-free carbonation of CA and formamide.[136] The emission and absorption in the NIR-I/II region gives these CDs excellent photothermal treatment capabilities. The NIR photons absorbed by CDs were converted into thermal energy under excitation at 808 nm (NIR-I) or 1064 nm (NIR-II). After CD injection, under laser irradiation at 808 nm or 1064 nm, the temperature of the tumor area rapidly rose to 52 °C, which is enough to cause irreversible damage to tumor tissue (Fig. 17a). The PTT efficacy of CDs was further assessed by monitoring the tumor growth rate and the tumor volume increased rapidly in the group treated with physiological saline and in the group treated with CDs without laser irradiation. In contrast, tumor growth was significantly slower under the 808 and 1064 nm laser irradiation (Fig. 17b–d). It could be observed that the tumor growth was inhibited, indicating that CDs can also be used as tumoricidal photothermal agents. Kim *et al.* prepared bio-excited CDs with strong NIR absorption from camellias flowers using a typical hydrothermal method.[137] It was observed that the low-dose of CDs (45 μg mL^{-1}) worked successfully and achieved an efficient PTT performance with a very high photothermal conversion efficiency (55.4%) at a medium laser power (808 nm, 1.1 W cm^{-2}) for safe and effective cancer treatment.

4.4 Synergistic therapy

Phototherapy, including PDT and PTT, has great potential for tumor diagnosis and treatment by inducing ROS or heat into the tumor. However, PDT or PTT has some limitations; for example, PTT requires prolonged and high-efficiency laser irradiation to generate sufficient heat. On the other hand, the hypoxic microenvironment of tumors and the limited diffusion distance of ROS hinder the efficacy of oxygen-dependent PDT. Since R-CD can induce the production of ROS from oxygen, water, *etc.*, under light irradiation and simultaneously convert absorbed light energy into heat, they can be used as both photosensitizers and photothermal agents in phototherapy.[138]

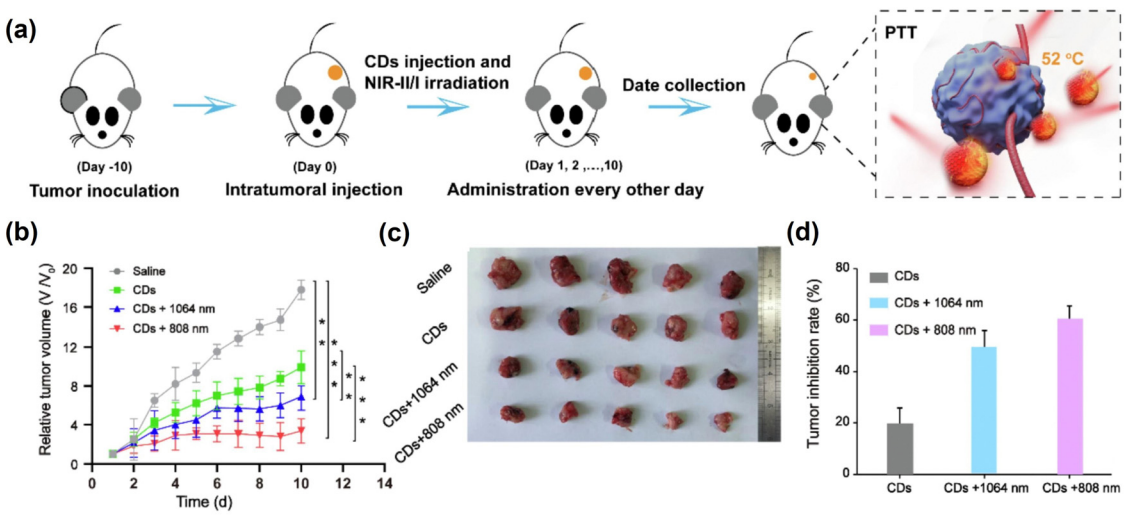

Fig. 17 (a) Treatment schedule on 4T1 tumor-bearing mice. (b) Relative tumor growth curves after CD treatment in mice. (c) Images of tumors in mice on the 10th day after treatment in different treatment groups. (d) Tumor inhibition rates of different treatment groups. Reprinted with permission from ref. 135 Copyright 2023, Elsevier.

Guo *et al.* used EDTA·2Na and $CuCl_2$ as raw materials, and then synthesized a new type of NIR-absorptive Cu, N-doped CDs (Cu, N-CDs) in a one-step hydrothermal method.[124] Cu^{2+} was located in the inner of Cu, N-CDs *via* N–Cu–N complexation, resulting in NIR absorption for producing heat and ROS. Cu, N-CDs significantly inhibited cancer *via* synergistic PTT/PDT. However, the presence of short wavelength absorption and emission, low ROS generation efficiency, and low photothermal conversion efficiency of most CDs have seriously hindered their application in the synergistic treatment of PDT and PTT for tumors. Therefore, there is still a need to put more effort into the preparation and modulation of photophysical and photochemical properties of the R-CDs. In recent years, researchers have gradually applied fluorescent CDs as intelligent materials for multimodal synergistic anticancer therapy. Zhang *et al.* obtained OCDs through one-step synthesis using citric acid and (1*R*,2*S*)-2-amino-1,2-diphenylethan-1-ol as substrates. OCDs exhibit excellent optical properties, typical AIE properties, and two-photon fluorescence imaging.[125] In addition, obsessive-compulsive disorder exhibits an excellent ability to produce type I ROS ($^{\bullet}OH$) with white light and good photothermal conversion ability under 808 nm irradiation. The generation of type I PDT ($^{\bullet}OH$) can trigger the transformation of protumoral M2 macrophages into antitumoral M1 macrophages, which exhibited an immunotherapy ability. The functions of AIE, two-photon imaging, PDT, and PTT enable OCDs to be used for multimodal combined therapy of tumors. Therefore, it can be seen that longer emission wavelengths and multimodal efficient treatment of tumors will become future research hotspots for further use in the *in vivo* system.

In addition to using PDT in combination with PTT, a combination of chemo-dynamic therapy (CDT) and PTT can also be used to treat cancer. Bai *et al.* developed NIR R-CDs using glutathione (GSH) as a precursor.[139] After R-CDs@MIL-100 entered the tumor microenvironment (TME), high concentrations of GSH reduced Fe^{3+} to Fe^{2+} and excreted GSH, triggering the release of the R-CDs and Fe^{2+}, at which point R-CD fluorescence was restored and turned 'on' to illuminate the tumor cells, thus enabling cancer imaging. The released Fe^{2+} reacted with the H_2O_2 in the TME to form highly reactive $^{\bullet}OH$ *via* the Fenton reaction, allowing CDT of tumors. Thus, efficient synergistic CDT/PTT bimodal treatment was achieved, guided by fluorescence imaging of the TME reaction. Bi's group also prepared Fe@EDTA-CDs with a core–shell structure by introducing Fe^{3+} for coordination with ethylenediamine tetraacetic acid (EDTA)-derived CDs, thus constructing a novel modular nanoplatform with both imaging and catalytic functions.[140] The spatial arrangement of the light-trapping chromophores and the catalytic sites in the Fe@EDTA-CDs can be resolved by discrete core–shell compartments, which gives rise to an interesting interaction and mutual reinforcement between each function. The synergistic shielding and stiffening effects induced by Fe coordinated core–shell structure increased the red-emission quantum yield, while the visible-light-promoted charge-transfer process could significantly enhance its catalytic activity. Thus, Fe@EDTA-CD showed a high ROS generation rate and light-enhanced anticancer efficiency, demonstrating the broad applications of CDs in CDT and PDT.

5. Conclusion & outlook

R-CDs are gaining popularity mainly due to their ability to show long wavelength emissions in the deep-red or NIR region. Scientists have discovered several ways to synthesize CDs containing predominantly red-emissive centers, which is expected to improve red emission of CDs with a low quantum yield in the long wavelength spectrum. Furthermore, surface engineering or post-modification treatments can be carried out to modulate PL emission of CDs, which can change the band gap of CQDs and convert their blue-emission into red-emission or enhance the quantum yield of R-CDs by reducing their surface defects. However, cost-effective approaches for large-scale production of blue- and green-emissive CDs can be achieved with high qualities such as high quantum yield, narrow emission and relatively low cost, but it's not as easy for the production of such high-quality R-CDs.

The review shows that R-CDs have been thoroughly examined regarding their synthetic methods, optical properties, and applications. In the specific preparation process, the simple and controllable synthesis methods for R-CDs mainly include: (a) adjusting the reaction conditions for the synthesis of CDs, including the feeding ratio of precursors, temperature, reaction time, solvent, and pH value of solution. (b) Heteroatom doping can effectively regulate the absorption and emission properties of R-CDs. The commonly used doping atoms are N, B, S, P and F, *etc.* (c) The optical properties of R-CD can also be regulated by surface passivation, self-assembly strategies and other chemical or physical methods. For example, CDs can self-assemble into "supra-CNDs" through electrostatic interactions or hydrogen bonds between CDs, and the supra-CNDs exhibited a new and strong absorption band at 700 nm.[141] (d) Above all, using advanced instruments, equipment, and technology to gain a clearer understanding of the synthesis mechanism and thus the generated structure of CDs. Many *in situ* monitoring techniques can effectively observe the formation process of CDs, providing strong support for the regulation of the optical properties of CDs, which is conducive to the efficient synthesis of R-CDs. However, some crucial issues still need to be addressed. The foremost challenge is controlling the R-CDs' structure, which determines their properties. Additionally, the PL emission mechanism of R-CDs is not yet clear, and it is necessary to conduct a systematic study by employing more advanced characterization techniques and theoretical simulations to determine the impact of parameters such as precursors, solvents, synthetic conditions, and doping elements on the luminescent properties of R-CDs. Moreover, exploring additional optical properties of R-CDs like up-conversion PL, long-reserved PL, or room-temperature phosphorescence is necessary to open new avenues for versatile applications.

In terms of prospects, the potential for the development of R-CDs in biological applications is enormous. Based on extensive studies of the structural properties of R-CDs, the design and synthesis of red/NIR-emitting CDs with excellent absorption in the long-wavelength region, physicochemical and biological properties are expected to further enable red/NIR-excited PDT of tumors in the clinic. Furthermore, photoimmunotherapy is a novel tumor treatment method that combines photodynamic therapy with immunotherapy. In this method, the patient is injected with a photosensitive drug that can combine with tumor cells, and the chemical reaction occurs under the red/near-infrared laser irradiation. These responses will destroy the structure of tumor cells and release a large amount of pro-inflammatory cytokines, thereby activating the cellular immune system to achieve efficient treatment of tumors. As above-mentioned, RNA-targeting R-CDs showed a prominent PDT effect against tumors cells through pyroptotic cell death,[122] which may provide a new approach to tumor photoimmunotherapy. As bio-imaging and drug-controlled release technologies continue to develop, R-CDs are expected to become an important nanomedicine or bionanomaterial contributing to early diagnosis, treating disease and improving human healthcare.[142] At the same time, with the development of new technologies and skills, the applications of R-CDs in biological fields will become more and more widespread.

Author contributions

For this review, W. X. Qin initiated the review concept and designed the manuscript contents; M. Y. Wang, Y. Li, L. C. Li, K. Abbas, Z. J. Li and A. C. Tedesco helped in the revision of the manuscript; H. B supervised the whole project. All the authors conjointly reviewed and edited the manuscript. All authors have read and agreed to the published version of the manuscript.

Conflicts of interest

There are no conflicts of interest to declare.

Acknowledgements

This work was financially supported by the National Natural Science Foundations of China (Grant No. 52172033, 51772001, and 22005280). We gratefully acknowledge the financial support from the National Key R&D Program of China (Grant No. 2021YFA1600202). We acknowledge support of the Key Laboratory of Structure and Functional Regulation of Hybrid Materials of Ministry of Education, Anhui University, Hefei, Anhui 230601, China. We also acknowledge support of the Key Laboratory of Environment Friendly Polymer Materials of Anhui Province, Hefei, China and Key Laboratory of Functional Inorganic Material Chemistry of Anhui Province, Anhui University, Hefei 230601, P. R. China.

Notes and references

1 B. W. Yao, H. Huang, Y. Liu and Z. H. Kang, Carbon dots: a small conundrum, *Trends Chem.*, 2019, **1**, 235–246.
2 C. L. Xia, S. J. Zhu, T. L. Feng, M. X. Yang and B. Yang, Evolution and synthesis of carbon dots: from carbon dots to carbonized polymer dots, *Adv. Sci.*, 2019, **6**, 1901316.
3 L. Dordevic, F. Arcudi, M. Cacioppo and M. Prato, A multifunctional chemical toolbox to engineer carbon dots for biomedical and energy applications, *Nat. Nanotechnol.*, 2022, **17**, 112–130.
4 H. Ding, J. S. Wei, P. Zhang, Z. Y. Zhou, Q. Y. Gao and H. M. Xiong, Solvent-controlled synthesis of highly luminescent carbon dots with a wide color gamut and narrowed emission peak widths, *Small*, 2018, **14**, 1800612.
5 A. Doring, E. Ushakova and A. L. Rogach, Chiral carbon dots: synthesis, optical properties, and emerging applications, *Light: Sci. Appl.*, 2022, **11**, 75.
6 K. J. Mintz, M. Bartoli, M. Rovere, Y. Zhou, S. D. Hettiarachchi, S. Paudyal, J. Chen, J. B. Domena, P. Y. Liyanage, R. Sampson, D. Khadka, R. R. Pandey, S. Huang, C. C. Chusuei, A. Tagliaferro and R. M. Leblanc, A deep investigation into the structure of carbon dots, *Carbon*, 2021, **173**, 433–447.
7 F. L. Yuan, S. H. Li, Z. T. Fan, X. Y. Meng, L. Z. Fan and S. H. Yang, Shining carbon dots: synthesis and biomedical and optoelectronic applications, *Nano Today*, 2016, **11**, 565–586.
8 Q. Wang, E. Pang, Q. X. Tan, S. J. Zhao, J. N. Yi, J. Zeng and M. H. Lan, Regulating photochemical properties of carbon dots for theranostic applications, *Wires Nanomed. Nanobi.*, 2023, **15**, e1862.
9 X. Xu, R. Ray, Y. Gu, H. J. Ploehn, L. Gearheart, K. Raker and W. A. Scrivens, Electrophoretic analysis and purification of fluorescent single-walled carbon nanotube fragments, *J. Am. Chem. Soc.*, 2004, **126**, 12736–12737.
10 Y. P. Sun, B. Zhou, Y. Lin, W. Wang, K. S. Fernando, P. Pathak, M. J. Meziani, B. A. Harruff, X. Wang, H. Wang, P. G. Luo, H. Yang, M. E. Kose, B. Chen, L. M. Veca and S. Y. Xie, Quantum-sized carbon dots for bright and colorful photoluminescence, *J. Am. Chem. Soc.*, 2006, **128**, 7756–7757.
11 H. Liu, T. Ye and C. Mao, Fluorescent carbon nanoparticles derived from candle soot, *Angew. Chem., Int. Ed.*, 2007, **46**, 6473–6475.
12 S. T. Yang, L. Cao, P. G. Luo, F. S. Lu, X. Wang, H. F. Wang, M. J. Meziani, Y. F. Liu, G. Qi and Y. P. Sun, Carbon dots for optical imaging *in vivo*, *J. Am. Chem. Soc.*, 2009, **131**, 11308–11309.
13 D. Xu, Q. L. Lin and H. T. Chang, Recent advances and sensing applications of carbon dots, *Small Methods*, 2020, **4**, 1900387.
14 S. Hu, A. Trinchi, P. Atkin and I. Cole, Tunable photoluminescence across the entire visible spectrum from carbon dots excited by white light, *Angew. Chem., Int. Ed.*, 2015, **54**, 2970–2974.
15 S. Zhu, Q. Meng, L. Wang, J. Zhang, Y. Song, H. Jin, K. Zhang, H. Sun, H. Wang and B. Yang, Highly

photoluminescent carbon dots for multicolor patterning, sensors, and bioimaging, *Angew. Chem., Int. Ed.*, 2013, **52**, 3953–3957.

16 Y. L. Hao, Z. X. Gan, J. Q. Xu, X. L. Wu and P. K. Chu, Poly(ethylene glycol)/carbon quantum dot composite solid films exhibiting intense and tunable blue–red emission, *Appl. Surf. Sci.*, 2014, **311**, 490–497.

17 D. Qu, Z. C. Sun, M. Zheng, J. Li, Y. Q. Zhang, G. Q. Zhang, H. F. Zhao, X. Y. Liu and Z. G. Xie, Three colors emission from S, N co-doped graphene quantum dots for visible light H_2 production and bioimaging, *Adv. Opt. Mater.*, 2015, **3**, 360–367.

18 K. Jiang, S. Sun, L. Zhang, Y. Lu, A. Wu, C. Cai and H. Lin, Red, green, and blue luminescence by carbon dots: full-color emission tuning and multicolor cellular imaging, *Angew. Chem., Int. Ed.*, 2015, **54**, 5360–5363.

19 F. L. Yuan, T. Yuan, L. Z. Sui, Z. B. Wang, Z. F. Xi, Y. C. Li, X. H. Li, L. Z. Fan, Z. A. Tan, A. M. Chen, M. X. Jin and S. H. Yang, Engineering triangular carbon quantum dots with unprecedented narrow bandwidth emission for multicolored LEDs, *Nat. Commun.*, 2018, **9**, 2249.

20 J. J. Liu, Y. J. Geng, D. W. Li, H. Yao, Z. P. Huo, Y. F. Li, K. Zhang, S. J. Zhu, H. T. Wei, W. Q. Xu, J. L. Jiang and B. Yang, Deep red emissive carbonized polymer dots with unprecedented narrow full width at half maximum, *Adv. Mater.*, 2020, **32**, 1906641.

21 Y. P. Liu, J. H. Lei, G. Wang, Z. M. Zhang, J. Wu, B. H. Zhang, H. Q. Zhang, E. S. Liu, L. M. Wang, T. M. Liu, G. C. Xing, D. F. Ouyang, C. X. Deng, Z. K. Tang and S. N. Qu, Toward strong near-infrared absorption/emission from carbon dots in aqueous media through solvothermal fusion of large conjugated perylene derivatives with post-surface engineering, *Adv. Sci.*, 2022, **9**, 2202283.

22 Y. X. Deng, Y. Y. Long, A. L. Song, H. Y. Wang, S. Xiang, Y. Qiu, X. Y. Ge, D. Golberg and Q. H. Weng, Boron dopants in red-emitting B and N co-doped carbon quantum dots enable targeted imaging of lysosomes, *ACS Appl. Mater. Interfaces*, 2023, **15**, 17045–17053.

23 L. Jiang, H. Cai, W. W. Zhou, Z. J. Li, L. Zhang and H. Bi, RNA-targeting carbon dots for live-cell imaging of granule dynamics, *Adv. Mater.*, 2023, **35**, 2210776.

24 H. Wang, J. Xu, Y. Q. Huang, H. L. Zhou, X. L. Fang, H. J. Li, X. Y. Wang and J. H. Yang, Red emissive carbon dots: photoluminescence mechanism, modulation and application research, *Chin. J. Lumin.*, 2020, **41**, 1579–1597.

25 W. Su, H. Wu, H. M. Xu, Y. Zhang, Y. C. Li, X. H. Li and L. Z. Fan, Carbon dots: a booming material for biomedical applications, *Mater. Chem. Front.*, 2020, **4**, 821–836.

26 J. J. Liu, R. Li and B. Yang, Carbon dots: a new type of carbon-based nanomaterial with wide applications, *ACS Cent. Sci.*, 2020, **6**, 2179–2195.

27 Y. Han, L. Liccardo, E. Moretti, H. G. Zhao and A. Vomiero, Synthesis, optical properties and applications of red/near-infrared carbon dots, *J. Mater. Chem. C*, 2022, **10**, 11827–11847.

28 J. Y. Wang, Y. H. Zhu and L. Wang, Synthesis and applications of red-emissive carbon dots, *Chem. Rec.*, 2019, **19**, 2083–2094.

29 D. Qu and Z. Sun, The formation mechanism and fluorophores of carbon dots synthesized via a bottom-up route, *Mater. Chem. Front.*, 2020, **4**, 400–420.

30 V. Sharma, P. Tiwari and S. M. Mobin, Sustainable carbon-dots: recent advances in green carbon dots for sensing and bioimaging, *J. Mater. Chem. B*, 2017, **5**, 8904–8924.

31 M. J. Yang, J. X. Shi, Y. Yin and C. G. Shi, Preparation of carbon nanodots with ultraviolet emission by pulsed laser ablation, *Phys. Status Solidi B*, 2021, **258**, 2100110.

32 H. Ming, Z. Ma, Y. Liu, K. M. Pan, H. Yu, F. Wang and Z. H. Kang, Large scale electrochemical synthesis of high-quality carbon nanodots and their photocatalytic property, *Dalton Trans.*, 2012, **41**, 9526–9531.

33 H. T. Li, X. D. He, Z. H. Kang, H. Huang, Y. Liu, J. L. Liu, S. Y. Lian, C. H. A. Tsang, X. B. Yang and S. T. Lee, Water-soluble fluorescent carbon quantum dots and photocatalyst design, *Angew. Chem., Int. Ed.*, 2010, **49**, 4430–4434.

34 J. Zhao, F. T. Li, S. Zhang, Y. An and S. Q. Sun, Preparation of N-doped yellow carbon dots and N, P co-doped red carbon dots for bioimaging and photodynamic therapy of tumors, *New J. Chem.*, 2019, **43**, 6332–6342.

35 S. Y. Lu, L. Z. Sui, J. J. Liu, S. J. Zhu, A. M. Chen, M. X. Jin and B. Yang, Near-infrared photoluminescent polymer–carbon nanodots with two-photon fluorescence, *Adv. Mater.*, 2017, **29**, 1603443.

36 Y. T. Meng, Y. Jiao, Y. Zhang, H. L. Zhang, X. J. Gong, Y. Liu, S. M. Shuang and C. Dong, One-step synthesis of red emission multifunctional carbon dots for label-free detection of berberine and curcumin and cell imaging, *Spectrochim. Acta, Part A*, 2021, **251**, 119432.

37 G. L. Ge, L. Li, D. Wang, M. J. Chen, Z. Y. Zeng, W. Xiong, X. Wu and C. Guo, Carbon dots: synthesis, properties and biomedical applications, *J. Mater. Chem. B*, 2021, **9**, 6553–6575.

38 J. Wang, J. Y. Wang, W. X. Xiao, Z. Geng, D. Tan, L. Wei, J. H. Li, L. J. Xue, X. B. Wang and J. T. Zhu, Lignin-derived red-emitting carbon dots for colorimetric and sensitive fluorometric detection of water in organic solvents, *Anal. Methods*, 2020, **12**, 3218–3224.

39 Q. W. Guan, R. G. Su, M. R. Zhang, R. Zhang, W. J. Li, D. Wang, M. Xu, L. Fei and Q. Xu, Highly fluorescent dual-emission red carbon dots and their applications in optoelectronic devices and water detection, *New J. Chem.*, 2019, **43**, 3050–3058.

40 H. Ding, X. X. Zhou, B. T. Qin, Z. Y. Zhou and Y. P. Zhao, Highly fluorescent near-infrared emitting carbon dots derived from lemon juice and its bioimaging application, *J. Lumin.*, 2019, **211**, 298–304.

41 T. V. de Medeiros, J. Manioudakis, F. Noun, J. R. Macairan, F. Victoria and R. Naccache, Microwave-assisted synthesis of carbon dots and their applications, *J. Mater. Chem. C*, 2019, **7**, 7175–7195.

42 X. Y. Lan, H. Ren, X. Yang, J. Wang, P. L. Gao and Y. Zhang, A facile microwave-assisted synthesis of highly crystalline

red carbon dots by adjusting the reaction solvent for white light-emitting diodes, *Nanotechnology*, 2020, **31**, 215704.

43 X. Y. Teng, C. G. Ma, C. J. Ge, M. Q. Yan, J. X. Yang, Y. Zhang, P. C. Morais and H. Bi, Green synthesis of nitrogen-doped carbon dots from konjac flour with ''off–on'' fluorescence by Fe3+ and L-lysine for bioimaging, *J. Mater. Chem. B*, 2014, **2**, 4631–4639.

44 X. X. Shi, H. M. Meng, Y. Q. Sun, L. B. Qu, Y. H. Lin, Z. H. Li and D. Du, Far-red to near-infrared carbon dots: preparation and applications in biotechnology, *Small*, 2019, **15**, 1901507.

45 Z. Y. Zhang, X. Y. Chen, G. C. Fang, J. J. Wu and A. L. Gao, Self-carbonization synthesis of highly-bright red/near-infrared carbon dots by solvent-free method, *J. Mater. Chem. C*, 2022, **10**, 3153–3162.

46 H. Sun, S. Xu, Z. Chen, F. Liu, S. Zong, Z. Wang and C. Wang, Solvent-free and dispersant-free synthesis of narrow full width at half maximum carbon dots via sole precursor of *p*-phenylenediamine, *Mater. Res. Bull.*, 2023, **159**, 112092.

47 L. Ai, Y. S. Yang, B. Y. Wang, J. B. Chang, Z. Y. Tang, B. Yang and S. Y. Lu, Insights into photoluminescence mechanisms of carbon dots: advances and perspectives, *Sci. Bull.*, 2021, **66**, 839–856.

48 S. S. Xue, P. F. Li, L. Sun, L. An, D. Qu, X. Y. Wang and Z. C. Sun, The formation process and mechanism of carbon dots prepared from aromatic compounds as precursors: a review, *Small*, 2023, **19**, 2206180.

49 B. Y. Wang, G. I. N. Waterhouse and S. Y. Lu, Carbon dots: mysterious past, vibrant present, and expansive future, *Trends Chem.*, 2023, **5**, 76–87.

50 S. Anwar, H. Z. Ding, M. S. Xu, X. L. Hu, Z. Z. Li, J. M. Wang, L. Liu, L. Jiang, D. Wang, C. Dong, M. Q. Yan, Q. Y. Wang and H. Bi, Recent advances in synthesis, optical properties, and biomedical applications of carbon dots, *ACS Appl. Bio Mater.*, 2019, **2**, 2317–2338.

51 F. Arshada and M. P. Sk, Aggregation-induced red shift in N, S-doped chiral carbon dot emissions for moisture sensing, *New J. Chem.*, 2019, **43**, 13240–13248.

52 F. Arshad, A. Pal and M. P. Sk, Review-aggregation-induced emission in carbon dots for potential applications, *ECS J. Solid State Sci. Technol.*, 2021, **10**, 021001.

53 Z. J. Zhu, Y. L. Zhai, Z. H. Li, P. Y. Zhu, S. Mao, C. Z. Zhu, D. Du, L. A. Belfiore, J. G. Tang and Y. H. Lin, Red carbon dots: optical property regulations and applications, *Mater. Today*, 2019, **30**, 52–79.

54 Y. F. Qu, D. Li and S. N. Qu, Solid-state luminescent carbon dots resistant to aggregation-induced fluorescence quenching: preparation, photophysical properties and applications, *Chin. J. Lumin*, 2021, **42**, 1141–1154.

55 Y. Q. Wang, X. C. Li, S. J. Zhao, B. H. Wang, X. Z. Song, J. F. Xiao and M. H. Lan, Synthesis strategies, luminescence mechanisms, and biomedical applications of near-infrared fluorescent carbon dots, *Coord. Chem. Rev.*, 2022, **470**, 214703.

56 X. Yang, L. Ai, J. K. Yu, G. I. N. Waterhouse, L. Z. Sui, J. Ding, B. W. Zhang, X. Yong and S. Y. Lu, Photoluminescence mechanisms of red-emissive carbon dots derived from non-conjugated molecules, *Sci. Bull.*, 2022, **67**, 1450–1457.

57 V. Bressi, A. M. Balu, D. Iannazzo and C. Espro, Recent advances in the synthesis of carbon dots from renewable biomass by high-efficient hydrothermal and microwave green approaches, *Curr. Opin. Green Sust.*, 2023, **40**, 100742.

58 M. Tariq, A. Singh, N. Varshney, S. K. Samanta and M. P. Sk, Biomass-derived carbon dots as an emergent antibacterial agent, *Mater. Today Commun.*, 2022, **33**, 104347.

59 N. Varshney, M. Tariq, F. Arshad and M. P. Sk, Biomass-derived carbon dots for efficient cleanup of oil spills, *J. Water Process Eng.*, 2022, **49**, 103016.

60 H. Ding, S. B. Yu, J. S. Wei and H. M. Xiong, Full-color light-emitting carbon dots with a surface-state-controlled luminescence mechanism, *ACS Nano*, 2016, **10**, 484–491.

61 B. H. Zhang, Z. Tian, D. Li, D. Zhou, X. Bao, Z. J. Zhu and S. N. Qu, Luminescent carbon dots: bandgap modulation and applications, *Chin. J. Lumin.*, 2019, **40**, 691–712.

62 S. J. Zhu, L. Wang, N. Zhou, X. H. Zhao, Y. B. Song, S. Maharjan, J. H. Zhang, L. J. Lu, H. Y. Wang and B. Yang, The crosslink enhanced emission (CEE) in non-conjugated polymer dots: from the photoluminescence mechanism to the cellular uptake mechanism and internalization, *Chem. Commun.*, 2014, **50**, 13845–13848.

63 S. J. Zhu, Y. B. Song, J. R. Shao, X. H. Zhao and B. Yang, Non-conjugated polymer dots with crosslink-enhanced emission in the absence of fluorophore units, *Angew. Chem., Int. Ed.*, 2015, **54**, 14626–14637.

64 S. Y. Tao, Y. B. Song, S. J. Zhu, J. R. Shao and B. Yang, A new type of polymer carbon dots with high quantum yield: from synthesis to investigation on fluorescence mechanism, *Polymer*, 2017, **116**, 472–478.

65 S. Y. Tao, S. Y. Lu, Y. J. Geng, S. J. Zhu, S. A. T. Redfern, Y. B. Song, T. L. Feng, W. Q. Xu and B. Yang, Design of metal-free polymer carbon dots: a new class of room-temperature phosphorescent materials, *Angew. Chem., Int. Ed.*, 2018, **57**, 2393–2398.

66 C. L. Xia, S. Y. Tao, S. J. Zhu, Y. B. Song, T. L. Feng, Q. S. Zeng, J. J. Liu and B. Yang, Hydrothermal addition polymerization for ultrahigh-yield carbonized polymer dots with room temperature phosphorescence via nanocomposite, *Chem. – Eur. J.*, 2018, **24**, 11303–11308.

67 S. Y. Tao, S. J. Zhu, T. L. Feng, C. Y. Zheng and B. Yang, Crosslink-enhanced emission effect on luminescence in polymers: advances and perspectives, *Angew. Chem., Int. Ed.*, 2020, **59**, 9826–9840.

68 S. Y. Tao, C. J. Zhou, C. Y. Kang, S. J. Zhu, T. L. Feng, S. T. Zhang, Z. Y. Ding, C. Y. Zheng, C. L. Xia and B. Yang, Confined-domain crosslink-enhanced emission effect in carbonized polymer dots, *Light: Sci. Appl.*, 2022, **11**, 56.

69 P. F. Li, S. S. Xue, L. Sun, X. P. Zong, L. An, D. Qu, X. Y. Wang and Z. C. Sun, Formation and fluorescent mechanism of red emissive carbon dots from *o*-phenylenediamine and catechol system, *Light: Sci. Appl.*, 2022, **11**, 298.

70 X. Miao, D. Qu, D. X. Yang, B. Nie, Y. K. Zhao, H. Y. Fan and Z. C. Sun, Synthesis of carbon dots with multiple color emission by controlled graphitization and surface functionalization, *Adv. Mater.*, 2018, **30**, 1704740.
71 Z. Tian, X. T. Zhang, D. Li, D. Zhou, P. T. Jing, D. Z. Shen, S. N. Qu, R. Zboril and A. L. Rogach, Full-color inorganic carbon dot phosphors for white-light-emitting diodes, *Adv. Opt. Mater.*, 2017, **5**, 1700416.
72 J. Zhan, B. J. Geng, K. Wu, G. Xu, L. Wang, R. Y. Guo, B. Lei, F. F. Zheng, D. Y. Pan and M. H. Wu, A solvent-engineered molecule fusion strategy for rational synthesis of carbon quantum dots with multicolor bandgap fluorescence, *Carbon*, 2018, **130**, 153–163.
73 P. Lesani, A. H. Mohamad Hadi, Z. F. Lu, S. Palomba, E. J. New and H. Zreiqat, Design principles and biological applications of red-emissive two-photon carbon dots, *Commun. Mater.*, 2021, **2**, 108.
74 W. X. Fan, J. He, H. Wei, C. Zhang, M. L. Zhu, D. F. Xu, S. Xiao, J. L. He, Z. H. Chen and J. Q. Meng, Broadband nonlinear optical properties of red fluorescent carbon dots, *Results Phys.*, 2022, **38**, 105591.
75 D. Li, P. T. Jing, L. H. Sun, Y. An, X. Y. Shan, X. H. Lu, D. Zhou, D. Han, D. Z. Shen, Y. C. Zhai, S. N. Qu, R. Zbořil and A. L. Rogach, Near-infrared excitation/emission and multiphoton-induced fluorescence of carbon dots, *Adv. Mater.*, 2018, **30**, 1705913.
76 S. Z. Yi, S. M. Deng, X. L. Guo, C. C. Pang, J. Y. Zeng, S. C. Ji, H. Liang, X. C. Shen and B. P. Jiang, Red emissive two-photon carbon dots: photodynamic therapy in combination with real-time dynamic monitoring for the nucleolus, *Carbon*, 2021, **182**, 155–166.
77 L. Jiang, H. Z. Ding, M. S. Xu, X. L. Hu, S. L. Li, M. Z. Zhang, Q. Zhang, Q. Y. Wang, S. Y. Lu, Y. P. Tian and H. Bi, UV-Vis-NIR full-range responsive carbon dots with large multiphoton absorption cross sections and deep-red fluorescence at nucleoli and *in vivo*, *Small*, 2020, **16**, 2000680.
78 K. K. Ng and G. Zheng, Molecular interactions in organic nanoparticles for phototheranostic applications, *Chem. Rev.*, 2015, **115**, 11012–11042.
79 Q. Feng, Z. G. Xie and M. Zheng, Color-tunable ultralong-lifetime room temperature phosphorescence with external heavy-atom effect in boron-doped carbon dots, *Chem. Eng. J.*, 2021, **420**, 127647.
80 K. Jiang, Y. H. Wang, C. Z. Cai and H. W. Lin, Conversion of carbon dots from fluorescence to ultralong room-temperature phosphorescence by heating for security applications, *Adv. Mater.*, 2018, **30**, 1800783.
81 F. Liu, Z. Y. Li, Y. Li, Y. Y. Feng and W. Feng, Room-temperature phosphorescent fluorine-nitrogen co-doped carbon dots: information encryption and anti-counterfeiting, *Carbon*, 2021, **181**, 9–15.
82 B. Wang, Y. Mu, H. Zhang, H. Shi, G. Chen, Y. Yu, Z. Yang, J. Li and J. Yu, Red room-temperature phosphorescence of CDs@zeolite composites triggered by heteroatoms in zeolite frameworks, *ACS Cent. Sci.*, 2019, **5**, 349–356.
83 W. Li, W. Zhou, Z. Zhou, H. Zhang, X. Zhang, J. Zhuang, Y. Liu, B. Lei and C. Hu, A universal strategy for activating the multicolor room-temperature afterglow of carbon dots in a boric acid matrix, *Angew. Chem., Int. Ed.*, 2019, **58**, 7278–7283.
84 K. T. Wang, L. J. Qu and C. L. Yang, Long-lived dynamic room temperature phosphorescence from carbon dots-based materials, *Small*, 2023, **19**, 2206429.
85 B. Bai, M. Xu, J. Z. Li, S. P. Zhang, C. Qiao, J. J. Liu and J. T. Zhang, Dopant diffusion equilibrium overcoming impurity loss of doped QDs for multimode anti-counterfeiting and encryption, *Adv. Funct. Mater.*, 2021, **31**, 2100286.
86 Y. F. Ding, X. L. Wang, M. Tang and H. B. Qiu, Tailored fabrication of carbon dot composites with full-color ultralong room-temperature phosphorescence for multidimensional encryption, *Adv. Sci.*, 2022, **9**, 2103833.
87 J. Tan, Q. J. Li, S. Meng, Y. C. Li, J. Yang, Y. X. Ye, Z. K. Tang, S. N. Qu and X. D. Ren, Time-dependent phosphorescence colors from carbon dots for advanced dynamic information encryption, *Adv. Mater.*, 2021, **33**, 2006781.
88 B. J. Geng, J. Y. Hu, Y. Li, S. N. Feng, D. Y. Pan, L. Y. Feng and L. X. Shen, Near-infrared phosphorescent carbon dots for sonodynamic precision tumor therapy, *Nat. Commun.*, 2022, **13**, 5735.
89 M. X. Lei, J. X. Zheng, Y. Z. Yang, L. P. Yan, X. G. Liu and B. S. Xu, Carbon dots-based delayed fluorescent materials: mechanism, structural regulation and application, *iScience*, 2022, **25**, 104884.
90 X. K. Chen, D. Kim and J. L. Brédas, Thermally activated delayed fluorescence (TADF) path toward efficient electroluminescence in purely organic materials: molecular level Insight, *Acc. Chem. Res.*, 2018, **51**, 2215–2224.
91 Y. Z. Shi, H. Wu, K. Wang, J. Yu, X. M. Ou and X. H. Zhang, Recent progress in thermally activated delayed fluorescence emitters for nondoped organic light-emitting diodes, *Chem. Sci.*, 2022, **13**, 3625–3651.
92 Q. Lou, N. Chen, J. Y. Zhu, K. K. Liu, C. Li, Y. S. Zhu, W. Xu, X. Chen, Z. J. Song, C. H. Liang, C. X. Shan and J. H. Hu, Thermally enhanced and long lifetime red TADF carbon dots via multi-confinement and phosphorescence assisted energy transfer, *Adv. Mater.*, 2023, **35**, 2211858.
93 D. Li, E. V. Ushakova, A. L. Rogach and S. N. Qu, Optical properties of carbon dots in the deep-red to near-infrared region are attractive for biomedical applications, *Small*, 2021, **17**, 2102325.
94 B. Y. Wang, H. J. Cai, G. I. N. Waterhouse, X. L. Qu, B. Yang and S. Y. Lu, Carbon dots in bioimaging, biosensing and therapeutics: a comprehensive review, *Small Sci.*, 2022, **2**, 2200012.
95 X. Sun and N. Mosleh, Fluorescent carbon dots for super-resolution microscopy, *Materials*, 2023, **16**, 890.
96 X. S. Yang, K. Zhanghao, H. Wang, Y. J. Liu, F. Wang, X. Zhang, K. B. Shi, J. T. Gao, D. Y. Jin and P. Xi, Versatile application of fluorescent quantum dot labels in super-resolution fluorescence microscopy, *ACS Photonics*, 2016, **3**, 1611–1618.
97 K. Warjurkar, S. Panda and V. Sharma, Red emissive carbon dots: a promising next-generation material with

intracellular applicability, *J. Mater. Chem. B*, 2023, **11**, 8848–8865.

98 Y. Y. Jing, G. Y. Liu, C. S. Zhang, B. Yu, J. Sun, D. Y. Lin and J. L. Qu, Lipophilic red-emitting carbon dots for detecting and tracking lipid droplets in live cells, *ACS Appl. Bio Mater.*, 2022, **5**, 1187–1193.

99 X. W. Hua, Y. W. Bao, J. Zeng and F. G. Wu, Nucleolus-targeted red emissive carbon dots with polarity-sensitive and excitation-independent fluorescence emission: high-resolution cell imaging and *in vivo* tracking, *ACS Appl. Mater. Interfaces*, 2019, **11**, 32647–32658.

100 K. F. Xu, H. R. Jia, Z. H. Wang, H. H. Feng, L. Y. Li, R. F. Zhang, S. Durrani, F. M. Lin and F. G. Wu, See the unseen: red-emissive carbon dots for visualizing the nucleolar structures in two model animals and *in vivo* drug toxicity, *Small*, 2023, **19**, 2205890.

101 B. Rathore, K. Sunwoo, P. Jangili, J. Kim, J. H. Kim, M. N. Huang, J. Xiong, A. Sharma, Z. G. Yang, J. Qu and J. S. Kim, Nanomaterial designing strategies related to cell lysosome and their biomedical applications: a review, *Biomaterials*, 2019, **211**, 25–47.

102 Y. Q. Sun, H. Y. Qin, X. Geng, R. Yang, L. B. Qu, A. N. Kani and Z. H. Li, Rational design of far-red to near-infrared emitting carbon dots for ultrafast lysosomal polarity imaging, *ACS Appl. Mater. Interfaces*, 2020, **12**, 31738–31744.

103 J. Y. Hu, R. Yang, H. Y. Qin, Y. Q. Sun, L. B. Qu and Z. H. Li, Spying on the polarity dynamics during wound healing of zebrafish by using rationally designed carbon dots, *Adv. Healthcare Mater.*, 2021, **10**, 2002268.

104 X. X. Wu, S. Sun, Y. H. Wang, J. L. Zhu, K. Jiang, Y. M. Leng, Q. H. Shu and H. W. Lin, A fluorescent carbon-dots-based mitochondria-targetable nanoprobe for peroxynitrite sensing in living cells, *Biosens. Bioelectron.*, 2017, **90**, 501–507.

105 Y. Zhang, C. J. Zhang, J. Chen, L. Liu, M. Y. Hu, J. Li and H. Bi, Trackable mitochondria-targeting nanomicellar loaded with doxorubicin for overcoming drug resistance, *ACS Appl. Mater. Interfaces*, 2017, **9**, 25152–25163.

106 N. Q. Gong, X. W. Ma, X. X. Ye, Q. F. Zhou, X. X. Chen, X. L. Tan, S. K. Yao, S. D. Huo, T. B. Zhang, S. Z. Chen, X. C. Teng, X. X. Hu, J. Yu, Y. L. Gan, H. D. Jiang, J. H. Li and X. J. Liang, Carbon-dot-supported atomically dispersed gold as a mitochondrial oxidative stress amplifier for cancer treatment, *Nat. Nanotechnol.*, 2019, **14**, 379–387.

107 Z. Zhu, C. L. Liu, X. M. Song, Q. X. Mao and T. Y. Ma, Carbon dots as an indicator of acid-base titration and a fluorescent probe for endoplasm reticulum imaging, *ACS Appl. Bio Mater.*, 2021, **4**, 3623–3629.

108 Y. X. Zhang, Q. Y. Jia, F. C. Nan, J. Wang, K. Liang, J. Li, X. K. Xue, H. H. Ren, W. M. Liu, J. C. Ge and P. F. Wang, Carbon dots nanophotosensitizers with tunable reactive oxygen species generation for mitochondrion-targeted type I/II photodynamic therapy, *Biomaterials*, 2023, **293**, 121953.

109 X. Zhang, L. Chen, Y. Y. Wei, J. L. Du, S. P. Yu, X. G. Liu, W. Liu, Y. J. Liu, Y. Z. Yang and Q. Li, Cyclooxygenase-2-targeting fluorescent carbon dots for the selective imaging of Golgi apparatus, *Dyes Pigm.*, 2022, **201**, 110213.

110 J. Kudr, L. Richtera, K. Xhaxhiu, D. Hynek, Z. Heger, O. Zitka and V. Adam, Carbon dots based FRET for the detection of DNA damage, *Biosens. Bioelectron.*, 2017, **92**, 133–139.

111 J. L. Wang, Y. F. Guo, X. Geng, J. Y. Hu, M. M. Yan, Y. Q. Sun, K. Zhang, L. B. Qu and Z. H. Li, Quantitative structure-activity relationship enables the rational design of lipid droplet-targeting carbon dots for visualizing bisphenol a-induced nonalcoholic fatty liver disease-like changes, *ACS Appl. Mater. Interfaces*, 2021, **13**, 44086–44095.

112 F. M. Lin, C. Y. Jia and F. G. Wu, Carbon dots for intracellular sensing, *Small Struct.*, 2022, **3**, 2200033.

113 J. T. Zhan, W. H. Song, E. X. Ge, L. X. Dai and W. L. Lin, Reversible fluorescent probes for biological dynamic imaging: current advances and future prospects, *Coord. Chem. Rev.*, 2023, **493**, 215321.

114 J. C. Ge, Q. Y. Jia, W. M. Liu, L. Guo, Q. Y. Liu, M. H. Lan, H. Y. Zhang, X. M. Meng and P. F. Wang, Red-emissive carbon dots for fluorescent, photoacoustic, and thermal theranostics in living mice, *Adv. Mater.*, 2015, **27**, 4169–4177.

115 M. Jiao, Y. X. Wang, W. J. Wang, X. Y. Zhou, J. Xu, Y. J. Xing, L. Chen, Y. Y. Zhang, M. H. Chen, K. Xu and S. H. Zheng, Gadolinium doped red-emissive carbon dots as targeted theranostic agents for fluorescence and MR imaging guided cancer phototherapy, *Chem. Eng. J.*, 2022, **440**, 135965.

116 T. Y. Luo, Y. Nie, J. Lu, Q. J. Bi, Z. Y. Cai, X. Song, H. Ai and R. R. Jin, Iron doped carbon dots based nanohybrids as a tetramodal imaging agent for gene delivery promotion and photothermal-chemodynamic cancer synergistic theranostics, *Mater. Des.*, 2021, **208**, 109878.

117 B. S. Tian, S. K. Liu, L. L. Feng, S. H. Liu, S. L. Gai, Y. L. Dai, L. S. Xie, B. Liu, P. P. Yang and Y. L. Zhao, Renal-clearable nickel-doped carbon dots with boosted photothermal conversion efficiency for multimodal imaging-guided cancer therapy in the second near-infrared biowindow, *Adv. Funct. Mater.*, 2021, **31**, 2100549.

118 W. Pang, P. F. Jiang, S. H. Ding, Z. Z. Bao, N. T. Wang, H. X. Wang, J. L. Qu, D. Wang, B. B. Gu and X. B. Wei, Nucleolus-targeted photodynamic anticancer therapy using renal-clearable carbon dots, *Adv. Healthcare Mater.*, 2020, **9**, 2000607.

119 M. H. Lan, S. J. Zhao, W. M. Liu, C. S. Lee, W. J. Zhang and P. F. Wang, Photosensitizers for photodynamic therapy, *Adv. Healthcare Mater.*, 2019, **8**, 1900132.

120 Y. L. Bai, J. J. Zhao, S. L. Wang, T. R. Lin, F. G. Ye and S. L. Zhao, Carbon dots with absorption red-shifting for two-photon fluorescence imaging of tumor tissue pH and synergistic phototherapy, *ACS Appl. Mater. Interfaces*, 2021, **13**, 35365–35375.

121 L. J. Li, J. Yang, J. H. Wei, C. H. Jiang, Z. Liu, B. Yang, B. Zhao and W. Song, SERS monitoring of photoinduced-enhanced oxidative stress amplifier on Au@carbon dots for tumor catalytic therapy, *Light: Sci. Appl.*, 2022, **11**, 286.

122 H. Cai, X. Y. Wu, L. Jiang, F. Yu, Y. X. Yang, Y. Li, X. Zhang, J. Liu, Z. J. Li and H. Bi, Lysosome-targeted carbon dots

with a light-controlled nitric oxide releasing property for enhanced photodynamic therapy, *Chin. Chem. Lett.*, 2023, 108946, DOI: 10.1016/j.cclet.2023.108946.

123 L. Jiang, H. Cai, W. X. Qin, Z. J. Li, L. Zhang and H. Bi, Meticulously designed carbon dots as photo-triggered RNA-destroyer for evoking pyroptosis, *Bioconjugate Chem.*, 2023, **34**, 1387–1397.

124 X. L. Guo, Z. Y. Ding, S. M. Deng, C. C. Wen, X. C. Shen, B. P. Jiang and H. Liang, A novel strategy of transition-metal doping to engineer absorption of carbon dots for near-infrared photothermal/photodynamic therapies, *Carbon*, 2018, **134**, 519–530.

125 Y. H. Zhang, H. Y. Xia, M. D. Yang, H. R. Li, F. S. Shan, Y. L. Chen, X. Yue, Z. Y. Wang and X. Q. Yu, Carbon dots with two-photon fluorescence imaging for efficient synergistic trimodal therapy, *Chin. Chem. Lett.*, 2023, **34**, 108197.

126 D. K. Ji, G. Reina, S. Guo, M. Eredia, P. Samorì, C. Ménard-Moyon and A. Bianco, Controlled functionalization of carbon nanodots for targeted intracellular production of reactive oxygen species, *Nanoscale Horiz.*, 2020, **5**, 1240–1249.

127 S. J. Zhao, K. Yang, L. R. Jiang, J. F. Xiao, B. H. Wang, L. T. Zeng, X. Z. Song and M. H. Lan, Polythiophene-based carbon dots for imaging-guided photodynamic therapy, *ACS Appl. Nano Mater.*, 2021, **4**, 10528–10533.

128 J. C. Ge, M. H. Lan, B. J. Zhou, W. M. Liu, L. Guo, H. Wang, Q. Y. Jia, G. L. Niu, X. Huang, H. Y. Zhou, X. M. Meng, P. F. Wang, C. S. Lee, W. J. Zhang and X. D. Han, A graphene quantum dot photodynamic therapy agent with high singlet oxygen generation, *Nat. Commun.*, 2014, **5**, 4596.

129 J. Q. Chen, C. Y. Ning, Z. N. Zhou, P. Yu, Y. Zhu, G. X. Tan and C. B. Mao, Nanomaterials as photothermal therapeutic agents, *Prog. Mater. Sci.*, 2019, **99**, 1–26.

130 H. J. Zhu, P. H. Cheng, P. Chen and K. Y. Pu, Recent progress in the development of near-infrared organic photothermal and photodynamic nanotherapeutics, *Biomater. Sci.*, 2018, **6**, 746–765.

131 X. Bao, Y. Yuan, J. Q. Chen, B. H. Zhang, D. Li, D. Zhou, P. T. Jing, G. Y. Xu, Y. L. Wang, K. Holá, D. Z. Shen, C. F. Wu, L. Song, C. B. Liu, R. Zbořil and S. N. Qu, *In vivo* theranostics with near-infrared-emitting carbon dots-highly efficient photothermal therapy based on passive targeting after intravenous administration, *Light: Sci. Appl.*, 2018, **7**, 91.

132 S. N. Qu, D. Zhou, D. Li, W. Y. Ji, P. T. Jing, D. Han, L. Liu, H. B. Zeng and D. Z. Shen, Toward efficient orange emissive carbon nanodots through conjugated sp^2-domain controlling and surface charges engineering, *Adv. Mater.*, 2016, **28**, 3516–3521.

133 J. C. Li, J. H. Rao and K. Y. Pu, Recent progress on semiconducting polymer nanoparticles for molecular imaging and cancer phototherapy, *Biomaterials*, 2018, **155**, 217–235.

134 Y. Lyu, Y. Fang, Q. Q. Miao, X. Zhen, D. Ding and K. Y. Pu, Intraparticle molecular orbital engineering of semiconducting polymer nanoparticles as amplified theranostics for *in vivo* photoacoustic imaging and photothermal therapy, *ACS Nano*, 2016, **10**, 4472–4481.

135 X. Zhen, C. Xie, Y. Y. Jiang, X. Z. Ai, B. G. Xing and K. Y. Pu, Semiconducting photothermal nanoagonist for remote-controlled specific cancer therapy, *Nano Lett.*, 2018, **18**, 1498–1505.

136 W. B. Zhao, D. D. Chen, K. K. Liu, Y. Wang, R. Zhou, S. Y. Song, F. K. Li, L. Z. Sui, Q. Lou, L. Hou and C. X. Shan, Near-infrared I/II emission and absorption carbon dots via constructing localized excited/charge transfer state for multiphoton imaging and photothermal therapy, *Chem. Eng. J.*, 2023, **452**, 139231.

137 D. Kim, G. Jo, Y. Chae, S. Subramani, B. Y. Lee, E. J. Kim, M. K. Ji, U. Sim and H. Hyun, Bioinspired camellia japonica carbon dots with high near-infrared absorbance for efficient photothermal cancer therapy, *Nanoscale*, 2021, **13**, 14426–14434.

138 B. L. Li, S. J. Zhao, L. Huang, Q. Wang, J. F. Xiao and M. H. Lan, Recent advances and prospects of carbon dots in phototherapy, *Chem. Eng. J.*, 2021, **408**, 127245.

139 Y. L. Bai, J. J. Zhao, L. L. Zhang, S. L. Wang, J. Hua, S. L. Zhao and H. Liang, A smart near-infrared carbon dot-metal organic framework assemblies for tumor microenvironment-activated cancer imaging and chemodynamic-photothermal combined therapy, *Adv. Healthcare Mater.*, 2022, **11**, 2102759.

140 X. Y. Wu, F. Yu, Y. F. Han, L. Jiang, Z. J. Li, J. F. Zhu, Q. Xu, A. Claudio Tedesco, J. W. Zhang and H. Bi, Enhanced chemodynamic and photoluminescence efficiencies of Fe–O_4 coordinated carbon dots *via* the core-shell synergistic effect, *Nanoscale*, 2023, **15**, 376–386.

141 D. Li, D. Han, S. N. Qu, L. Liu, P. T. Jing, D. Zhou, W. Y. Ji, X. Y. Wang, T. F. Zhang and D. Z. Shen, Supra-(carbon nanodots) with a strong visible to near-infrared absorption band and efficient photothermal conversion, *Light: Sci. Appl.*, 2016, **5**, e16120.

142 M. Ortega-Muňoz, P. Vargas-Navarro, S. Plesselova, M. D. Giron-Gonzalez, G. R. Iglesias, R. Salto-Gonzalez, F. Hernandez-Mateo, A. V. Delgado, F. J. Lopez-Jaramillo and F. Santoyo-Gonzalez, Amphiphilic-like carbon dots as antitumoral drug vehicles and phototherapeutical agents, *Mater. Chem. Front.*, 2021, **5**, 8151.